High-Temperature Ceramic Silver Paste Connectors: Fabrication and Performance Analysis

by

CYNDERILA C. PATRICK

Submitted in Partial Fulfillment of the

Requirements for the Degree of

Master of Science

in the

Chemical Engineering

High-Temperature Ceramic Silver Connectors: Fabrication and Performance Analysis

Cynderila C. Patrick

I hereby release this thesis to the public. I understand that this thesis will be made available from the OhioLINK ETD Center and the Maag Library Circulation Desk for public access. I also authorize the University or other individuals to make copies of this thesis as needed for scholarly research.

Signature:

Cynderila C. Patrick, Student — Date

Approvals:

Dr. Holly Martin, Thesis Advisor — Date

Dr. Frank Li, Committee Member — Date

Dr. Byung-Wook Park, Committee Member — Date

Dr. Sal Sanders Dean of Graduate Studies — Date

ABSTRACT

Advanced materials with desired capabilities are needed for electronics intended for extreme environments. These environments will likely include high temperatures, high pressures, and thermal or mechanical shock. Ceramics have been integral to human civilization for millennia, offering versatility and functionality across diverse applications. In the realm of advanced technologies, ceramics play a pivotal role, especially in electronics, automotive, and aerospace industries. This research revolves around the fabrication and performance analysis of high-temperature ceramic silver connectors, aiming to enhance their functionality and reliability in demanding electronic applications. The pursuit of high-temperature ceramic materials for advanced electronic applications has prompted extensive research and experimentation, aiming to blend the benefits of ceramic materials and additive manufacturing (AM) processes. In this study, a systematic investigation to fabricate and evaluate silver ceramic connectors, focusing on optimizing their durability, electrical conductivity, and thermal resilience, was conducted. Employing AM manufacturing techniques, ceramic substrates were meticulously fabricated using photopolymer resin infused with silica-filled ceramic particles. Subsequently, silver conductive designs were deposited onto the ceramic substrates utilizing specialized silver conductive paste employing Voltera V-One printer.

The findings from resistance and resistivity measurements confirmed the suitability of these connectors for high-temperature use. Conductivity tests revealed that the SCC-3 (triple printed) silver ceramic connector exhibited the lowest resistance to current flow, indicating superior electrical properties compared to other connectors. While dense coatings may enhance performance, they also necessitate more resources and time during manufacturing. Additionally, connectors cured at higher temperatures (400°C) demonstrated improved electrical conductance compared to those cured at lower temperatures, crucial for applications requiring high temperature

stability, like automotive and aerospace industries. The specific properties of high temperature ceramic silver paste connectors may vary depending on materials and manufacturing processes, suggesting that engineers and manufacturers must weigh factors such as printing frequency, material cost, production time, and desired conductivity levels.

Adhesion tests demonstrated bonding between ceramic and silver components, particularly evident in SCC-2 (double printed) compared to SCC-1 (single printed), ensuring mechanical integrity and durability. The results underscore the importance of achieving consistent and robust adhesive bonds in high-temperature ceramic silver connectors. Variations in adhesion strength between SCC-1 and SCC-2 samples emphasize the influence of printing parameters on adhesive bonding. These findings highlight the necessity for meticulous control and optimization of fabrication processes to ensure reliable connector performance in real-world applications.

In conclusion, the findings presented herein provide an assessment of the fabrication and evaluation of high-temperature ceramic silver connectors. These connectors hold significant promise for a wide array of high-temperature electronic applications, spanning industries including automotive, aerospace, defense, automotive and energy sectors. The insights obtained from this study contribute to the ongoing advancement of ceramic-based passive components and system integration in high-power electronics, paving the way for enhanced performance and reliability in demanding operating environments.

ACKNOWLEDGEMENTS

I would like to extend my heartfelt appreciation to all individuals who have made valuable contributions towards the successful completion of this thesis. First and foremost, I am deeply indebted to my supervisor **Prof. Dr. Martin**, whose guidance, support, and invaluable insights have been instrumental throughout this research journey. Your patience, encouragement, and unwavering support helped me tremendously to complete this thesis.

I extend my heartfelt appreciation to the faculty members and staff of Youngstown State University, whose expertise, encouragement, and resources have enriched my academic experience and facilitated the completion of this thesis. I would like to thank my friends for their camaraderie, support, and encouragement during challenging times. Your friendship and camaraderie have made this academic journey more enjoyable and memorable.

Last but not the least, I am deeply thankful to my family for their unwavering love, encouragement, and understanding throughout this endeavor. Your unwavering support and belief in me have been my source of strength and motivation.

This thesis owes its existence to the combined endeavors, assistance, and motivation provided by all the individuals named earlier. I express my gratitude for your participation in this endeavor and for assisting me in reaching this significant accomplishment in my academic journey.

Cynderilla

List of Acronyms

AM – Additive Manufacturing

SLA – Stereo Lithography

VPP – Vat Phot Polymerization

MJ – Material Jetting

CIM – Ceramic Injection Molding

BJP – Binder Jetting Printing

CAD – Computer Aided Design

SEM – Scanning Electron Microscope

LPS – Liquid Phase Sintering

SiO_2 – Silicon Dioxide / Silica

Al_2O_3 – Aluminum Oxide / Alumina

ZrO_2 – Zirconium Dioxide / Zirconia

SiC – Silicon Carbide

3D: Three-Dimensional

V-One – Voltera V-One

CLIP – Continuous Liquid Interface Production

DLP – Digital Light Processing

ISO – International Organization for Standardization

UV – Ultraviolet

IPA – Isopropyl Alcohol

SCC-1 – Silver Ceramic Connector (Single print)

SCC-2 – Silver Ceramic Connector (Double print)

SCC-3 – Silver Ceramic Connector (Tingle print)

Table of Contents

Abstract…………………….. …iii
List of Figures………..ix
List of Tables………..xi
CHAPTER 1 INTRODUCTION..……..……….1
1.1. Background………...1
1.2. Additive Manufacturing of Ceramics 8
CHAPTER 2 LITERATURE REVIEW 12
2. Introduction……... 12
2.1. Traditional Vs Advanced Ceramics Manufacturing 14
2.2. Advanced Manufacturing of Ceramics 16
2.2.1. Powder-based Deposition Techniques 21
2.2.2. Bulk-Solid Based Deposition Techniques 26
2.2.3.Slurry-Based Deposition Techniques..28
2.3. Ceramic Metal Connectors 31
2.4. High Temperature Co-fired and Low Temperature Co-fired Ceramic..32
2.5. Research Problem Statement 35
CHAPTER 3 METHODOLOGY 38
3. Introduction…….. 38
3.1. Materials…………. 38
3.2. Equipment & Software 38
3.3. Manufacturing of Silver Ceramic Connectors...39
3.3.1. Printing of Ceramic Substrates 40
3.3.2. Sintering…………..41
3.4. Printing of Silver Conductive Designs 43
3.4.1. Preparation of Silver Paste...43
3.4.2. Deposition of Silver Paste 43
3.5. Characterization of Silver Conductive Connectors 44
3.5.1. Conductivity Testing 44
3.5.2. Adhesion Testing..44
CHAPTER 4 RESULTS AND DISCUSSION 46
4. Introduction……… 46
4.1.Printing of Conductive Silver Paste on Ceramics..46
4.2. Conductivity of the Printed Silver paste 49

4.3. Adhesion Testing of Conductive silver paste on Ceramic..54
4.4. Adhesion Results Analysis 55
5. Discussion…………..56
CHAPTER 5 CONCLUSIONS AND RECOMMENDATIONS……………..59
5.1. Recommendations 60
References……………. 62

List of Figures

Figure 1.1. Strength plotted against density in a classical Ashby diagram illustrating relative strength of various materials with ceramics being at the top………………………………………………………...3

Figure 1.2. Diagrams showing the (a) various types of ceramic materials; (b) Some of the prominent fields in which advanced ceramics are being applied…………………………………………………………..4

Figure 1.3. Schematic diagram of the ceramic part fabrication……………………………...…………..6

Figure 1.4. Advanced ceramics market size, growth trends 2021-2029…………………………………....7

Figure 1.5. Diagram showing the various steps to produce advanced ceramic materials via AM. The typical operational steps relate to Stereolithography (SL) & Digital Light Processing (DLP) processes...10

Figure 2.1. Conventional ceramic manufacturing methods and high-value added manufacturing………16

Figure 2.2. A timeline of important developments in AM technology from 1980s to 2018………………17

Figure 2.3. (A) Diagram of the vat photopolymerization technology, which produces 3D components by selectively curing layer by layer a photocurable resin. (B) Light scattering causes overexposure in particle suspensions with large loads. (C, D) Post-processing resulted in dense zirconia specimens with complicated shape and no obvious layer interfaces……………………………………………………18

Figure 2.4 A schematic showing the direct and indirect modes of additive manufacturing. Sintering and pyrolysis are mandatory steps when proceeded via indirect AM………………………………………19

Figure 2.5. The diagram shows the schematic representation of various additive manufacturing processes. (a) Stereolithography (SL) process, (b) Digital Light Processing (DLP) process, (c) Two-Photon Polymerization (TPP) process, (d) Inkjet Printing (IJP) process, with inset showing droplets being jetted from the printhead at higher magnification. (e) Direct Ink Writing (DIW) process, with inset showing a nozzle extruding ceramic feedstock. (f) Three-Dimensional Printing (3DP) process, with inset showing the printhead jetting a binder solution. The SLS method includes Selective Laser Melting (SLM) and the LOM process.…………………………………………...……………………………………....20

Figure 2.6. (a) MicroCT image of three samples (d) percentage of porosity, (e) the flexural strength of the L-PBF-printed spodumene-Al_2O_3 samples at various temperatures……………………………………………..……………………………………..24

Figure 2.7. SEM images related to barium titanate after being sintered at (a & b) 1260 °C; (c & d) 1330 °C; (e & f) 1400 °C for 4 h………………………………………………………………………..25

Figure 2.8. BCP/ZrO_2 scaffold SEM images: (a) approximately 350 µm pore size as well as 500 µm printed lattice breadth; (b) granular interface of the FDM-manufactured structure following printing along with sintering………………………………………………………………………………………27

Figure 2.9. Comparing the relative energy applied, speed of the additive manufacturing process, and resolution of created items utilizing seven primary types of additive manufacturing processes……........29

Figure 2.10. LTCC circuit board production cycle……….…………………………………………….33

Figure 3.1. Flow diagram showing the 2 distinct processes for the fabrication of silver ceramic connectors along with their characterization by various techniques……………………………………………………..39

Figure 3.2. Diagram showing the sintering process……………………………………………………….41

Figure 3.3. Graph showing the temperature variation profile during sintering process…………………..43

Figure 4.1. Images showing the printed silver paste conductive design on ceramic (a) SCC-1, (b) SCC-2, and (c) SCC-3……………………………………………………………………………………………...48

Figure 4.2 Relationship between (a) Resistance vs Length, (b) Resistivity vs Length of SCC-1….……..49

Figure 4.3 Graph showing the (a) resistance vs length and (b) resistivity vs length trend for SCC-1 to SCC-3……………………………………………………………………………………………………...52

Figure 4.4. Graph showing the trent lines for resistance vs distance for SCC-1 cured at three different temperatures……………………………………………………………………………………………….53

Figure 4.6. Setup of Adhesion Apparatus………………………………………………………………....54

Figure 4.7. Adhesion analysis of SCC-1 and SCC-2……………………………………………………...55

Figure 4.8: Results of Adhesion Test……………………………………………………………………...56

List of Tables

Table 1.1. The global ceramics market size dynamics…………………………………………………..6

Table 2.1. Chemical as well as physical properties of HTCC components……………………………….34

Table 3.1. Sintering parameters employed in this study in air at 1 atm…………………………………...42

Table 4.1. Resistance vs distance values for all the three samples i.e. SCC-1 to SCC-3…………………51

Table 4.2. Resistance vs distance values for SCC-1 cured at three different temperatures……………….53

CHAPTER 1 INTRODUCTION

1.1. Background

Ceramics, one of humanity's oldest and most versatile materials, has been part of our lives for thousands of years. From the simple clay pots of ancient civilizations to the sleek porcelain of today's modern designs, ceramics have always been with us [1]. They're not just decorative; ceramics also play crucial roles in advanced technologies like electronics, automotive industry, and medicine, among many others. Ceramics boasts a storied legacy spanning civilizations. Originating in ancient Mesopotamia around 10,000 BCE, ceramics quickly became indispensable to daily life, facilitating food storage, cooking, and trade [2].

The term ceramic comes from the Greek word called keramikos (κεραμοσ) meaning "of pottery" [3]. Ceramics are often composed of 2 or 3 elements, with oxygen, carbon, boron, and nitrogen being the most prevalent compositions. Chemically, the majority of ceramics are held together by ionic or covalent bonds. As a result, these compounds have intrinsic hardness and brittleness. Ceramics have great resistance, as well as robust thermal properties, when fired at temperatures of, or exceeding, 1000˚C. Moreover, ceramics are distinguished by qualities such as strength and hardness, electrical conductivity and temperature resistance, chemical inactivity, and non-magnetic nature [4].

Ceramics provide great thermal insulation and mechanical qualities throughout a wide temperature range. Furthermore, their outstanding electrical insulating qualities have led to an increase in their application in electronics production. Ceramic materials also have low thermal expansion coefficients, allowing them to expand negligibly with temperature changes while maintaining high form consistency [5]. They are highly dense materials having strength greater than polymers, elastomers, and foams, but only second to metals. Figure 1.1. shows classical Ashby diagram illustrating density (x-axis) and strength (y-axis) profiles of various

materials. As is evident from Figure 1.1. some special ceramics including aluminum oxide (Al_2O_3) and silicon carbide (SiC) show the highest strength and are often used in applications requiring durability and resistance to high temperatures. Thus, ceramics attract a lot of attention in several industrial applications, including automotive, aerospace, and machine tools, because of the remarkable mechanical properties, which include high-temperature strength, corrosion resistance, good wear resistance, viable optical properties, chemical stability, and good tribological properties [6]. Ceramics, integral to various industries and everyday life, exhibit remarkable diversity and utility, often categorized into five distinct categories based on their chemical compositions and properties. Glasses are the first type, are predominantly comprised of silica (SiO_2), and are widely utilized in household items, like Pyrex cookware, borosilicate glassware, and architectural elements, like windowpanes, owing to their transparency and thermal resistance [7]. Vitreous ceramics, rooted in clay, are the second type and form the backbone of traditional ceramic products, such as cutlery, pipes, bricks, and tiles, offering durability and versatility in construction and domestic settings [8]. High-performance ceramics, incorporating oxides, borides, nitrides, and carbides, are the third type and are engineered for demanding applications necessitating superior fracture toughness and wear resistance, with uses in aerospace components, cutting tools, and biomedical implants [9]. Cement and concrete, which are complex ceramic amalgams of lime, silica, and alumina, are the fourth type and are considered the cornerstone of civil engineering projects, serving as the primary binding agents and structural materials in buildings, roads, and infrastructure [10]. Lastly, the fifth type is natural ceramics, occurring as rocks and minerals, showcase geological significance and contribute to geological formations, mineral resources, and Earth's crust composition, demonstrating the intricate interplay between ceramics and the natural world [11]. Each category of ceramics underscores the breadth of their applications, ranging from utilitarian necessities to cutting-edge innovations, underscoring their enduring relevance in modern society.

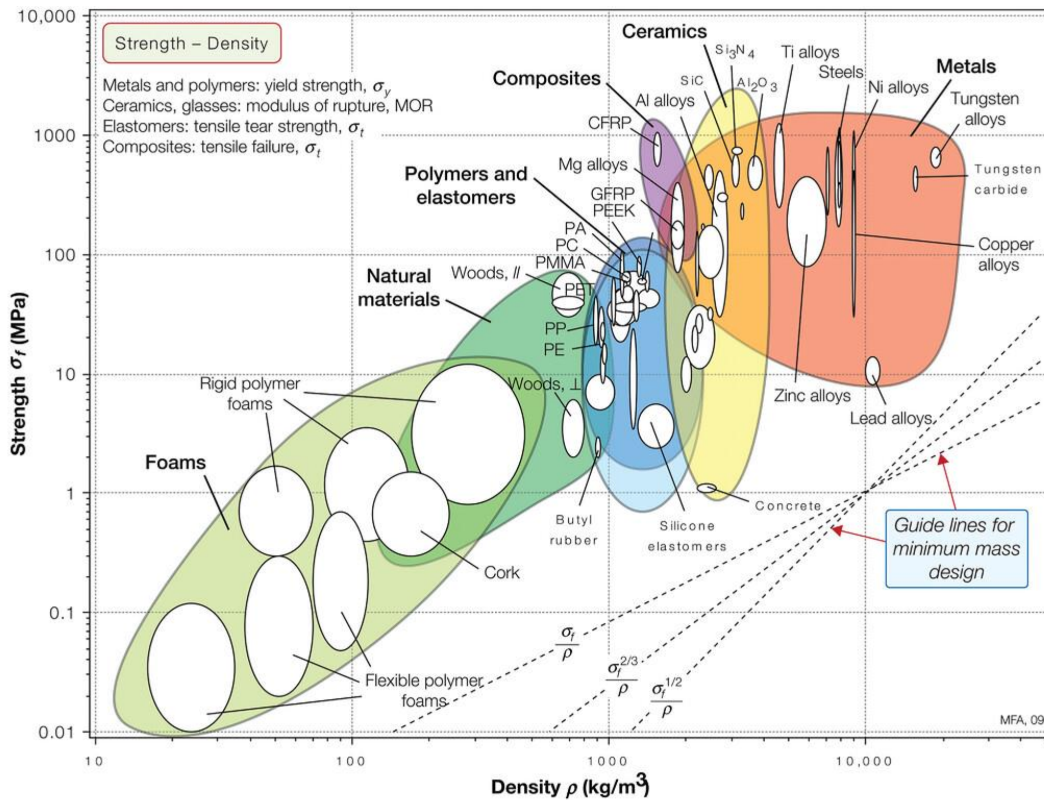

Figure 1.1. *Strength plotted against density in a classical Ashby diagram illustrating relative strength of various materials with ceramics being at the top [12].*

Based on their applicability, ceramics could be classified into 2 main sections, traditional ceramics and advanced ceramics. Figure 1.2a shows a detailed classification of ceramics into traditional and advanced ceramics. Several types of traditional ceramics including abrasives, adhesives, refractories, cement, and clay products etc. are included in this category while advanced ceramics are further classified into structural and functional ceramics. Advanced ceramics differ from traditional ceramics in terms of thermal conduction, wear resistance, and mechanical performance at elevated temperatures. As a result, advanced ceramics are employed in places that demand great strength, including wear resistance in extreme temperatures. A good weight-to-strength ratio pertains to the most essential attribute displayed by such technological ceramics. Traditional ceramics are primarily composed of clay minerals and other natural raw materials. They undergo shaping and firing processes to

achieve their final form. For example, earthenware, stoneware, and porcelain are crafted using traditional pottery techniques. Clay-based bricks and tiles have been integral to construction for centuries. They provide structural support, insulation, and decorative elements in buildings worldwide. Refractory materials, such as firebricks and kiln linings, withstand high temperatures and harsh chemical environments. They find use in furnaces, kilns, and industrial processes [8].

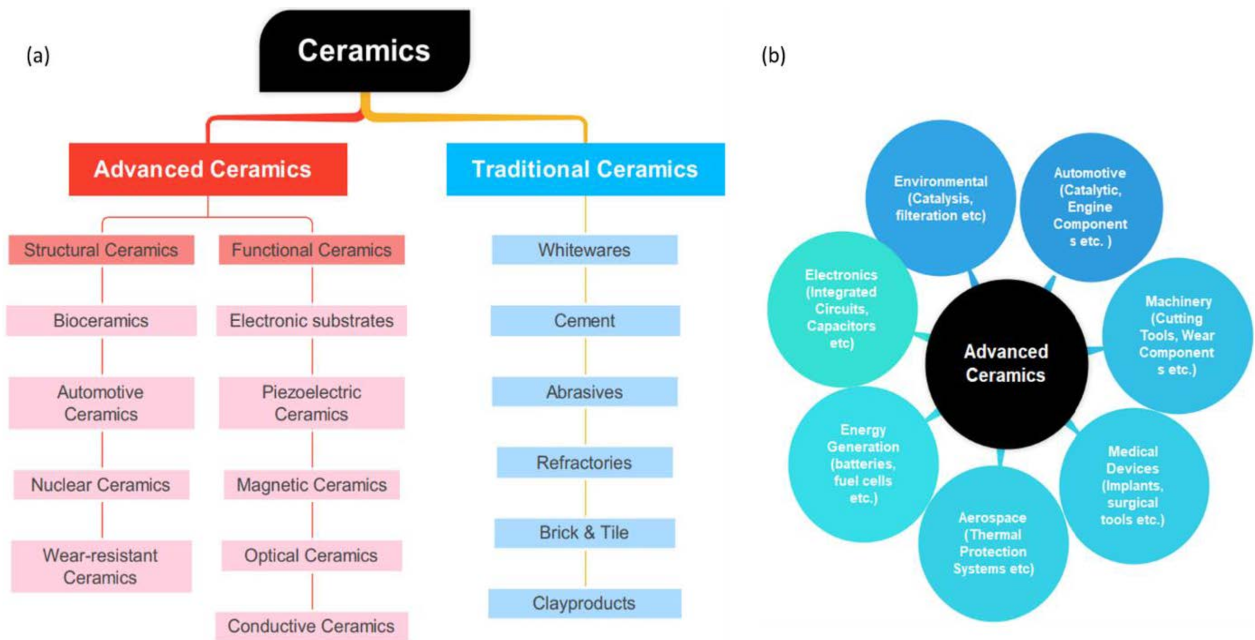

Figure 1.2. *Diagrams showing the* **(a)** *various types of ceramic materials;* **(b)** *Some of the prominent fields in which advanced ceramics are being applied.*

Advanced ceramics, also called technical ceramics, engineering ceramics, high-tech ceramics, or fine ceramics, encompass a broad array of high-performance materials. These are essentially crystalline materials with rigorously streamlined compositions that are created under strict regulations from highly refined or described raw components that provide exactly defined properties. Advanced ceramic components are prepared by treatment of ceramic powders, which require careful treatment to manage particle size, heterogeneity, purity, particle size distribution (PSD), and chemical compositions. [13]. The aforementioned

parameters influence the characteristics of final ceramic components and thus offer exceptional mechanical, thermal, and electrical properties. Figure 1.2b shows an overview of some of the most prominent fields in which advanced ceramics are being applied.

For instance, alumina (Al_2O_3) ceramics exhibit wear resistance, high hardness, and chemical stability. They are used in cutting tools, ball bearings, and biomedical implants. Zirconia (ZrO_2) ceramics possess superior strength, toughness, and thermal shock resistance. They are utilized in dental crowns, hip implants, and structural components. Silicon carbide (SiC) ceramics boast exceptional hardness, thermal conductivity, and corrosion resistance. They find applications in armor plates, brake discs, and electronic devices [14]. Titanium dioxide (TiO_2) ceramics are valued for their optical properties, including high refractive index and opacity. They are employed in pigment production, sunscreen formulations, and photocatalysis. High Performance Ceramics (e.g. silicon carbide, zirconia, boron nitride, silicon nitride) are promising materials for mechanical, as well as chemical resistance, applications in hostile environments. These sophisticated engineered ceramics can withstand tremendous temperatures (1400°C and more) while maintaining great mechanical strength [15].

Ceramic components can be treated in 4 different steps: preparation of material, processing, burning, and finishing. A scheme of manufacturing process for ceramic part is shown in Figure 1.3. Here, conventional ceramic components are processed using a variety of methods, including direct foaming, wet forming, dry forming, thixotropic casting, gel-casting, phase inversion, and freeze casting [16]. Sintering the green parts at elevated temperatures is also needed to obtain densification, a process that involves the particles of a ceramic material being fused together resulting in increased density and strength and reduction of porosity. However, such ceramic forming processes have limits because of lengthy processing times and high prices.

Figure 1.3. *Schematic diagram of the ceramic part fabrication.*

The worldwide market size of ceramics has been estimated to be $133.7 billion USD for the year 2024 (see Table 1.1 for growth in the US and worldwide) and the projections expect it to be close to $240 billion USD at the end of 2034 with a CAGR of 6% [17]. Increasing demand for advanced ceramics in the medical field, as well as increased use in the military industry, are key drivers of market revenue development.

Table 1.1. *The global ceramics market size dynamics [17].*

Report Attributes	**Details**
Ceramics Market Size (2024)	US$ 133.7 Billion
Projected Market Value (2034F)	US$ 240 Billion
Global Market Growth Rate (2024 to 2034)	6% CAGR
East Asia and South Asia & Oceania Market Share (2023)	~40%
Demand Growth in Europe (2024 to 2034)	6.3% CAGR
Traditional Ceramics Segment Share (2023)	>50%

The market in the United States is driven by the electronics sector, where advanced ceramics are employed in numerous applications, such as substrates, circuit carriers, core materials, and other components. In 2021, North America had the biggest revenue chunk of the worldwide advanced ceramics market (see Fig. 1.4 for detailed market size and growth trends) [18]. It is owing to increased demand in a variety of end-use industries, including construction and infrastructure, in the Canada and the United States [18].

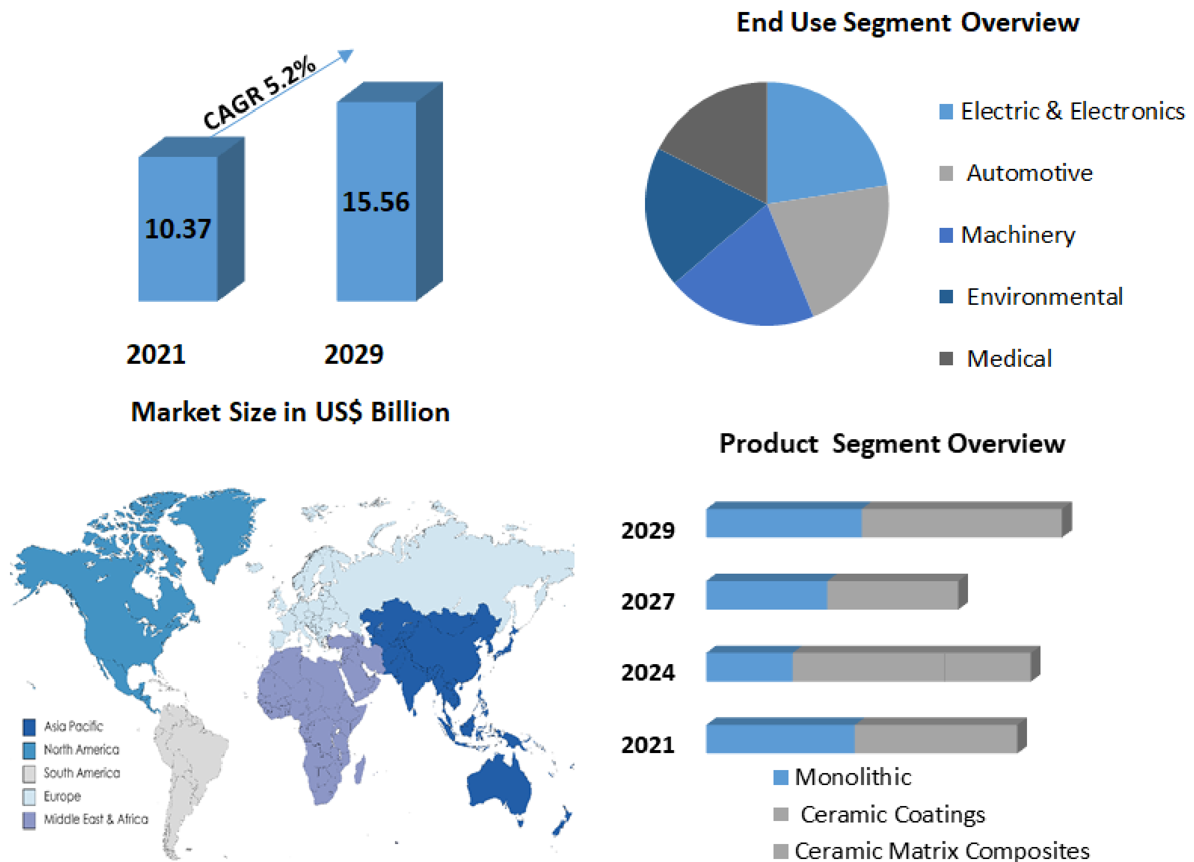

Figure 1.4. *Advanced ceramics market size, growth trends 2021-2029 [19].*

The worldwide advanced ceramics market is divided into seven material categories: Zirconate (ZrO_2), alumina (Al_2O_3), titanate (TiO_2), aluminum nitride (AlN), ferrite (Fe_2O_3), silicon carbide (SiC), and silicon nitride (Si_3N_4).

The alumina category had the largest revenue chunk in the worldwide advanced ceramics market, as of 2021. However, based on the product, the worldwide advanced ceramics market is divided into three product segments: ceramic coatings, monolithic, and ceramic matrix composites [20]. Ceramic coatings are thin layers applied to surfaces to improve properties like wear and corrosion resistance. Monolithic ceramics are solid pieces without internal reinforcement, widely used in industries for applications such as electrical insulation and structural components. Ceramic matrix composites (CMCs) are composite materials combining a ceramic matrix with reinforcements like fibers or particles, offering superior

strength and thermal resistance, commonly employed in aerospace and automotive applications. Over the forecast period, the monolithic category is predicted to develop the quickest in the worldwide advanced ceramics market in terms of revenue, as shown in Figure 1.4. Monolithic capacitors, a critical ingredient of electronics sector, are being employed in a variety of electronic production processes and electronic machinery, propelling revenue growth in this category [21].

1.2.Additive Manufacturing of Ceramics

Although substantial progress has been made regarding the fabrication of advanced ceramics with better properties, most difficult limitations are the constraints imposed by geometrical design and structural complexity of ceramics, given the high-performance applications in the fields of electronics, aerospace, energy, and defense. Nonetheless, fabricating complicated ceramic components is challenging, and mold production processes are expensive, as well as time-consuming, and use traditional forming procedures, including dry pressing, tape casting, isostatic pressing, and gel-casting. [22].

Consequently, in order to produce high-performance ceramic elements with intricate geometries, a novel forming technique is required. The advancement of additive manufacturing (AM), also referred to as three-dimensional (3D) printing, is regarded as an industrial revolution [23]. Using 3D CAD models that have been cut digitally into two dimensional cross sections, a variety of physical components in a distinct point-by-point, or layer-by-layer additive way are produced. A revolutionary approach to manufacturing, 3D printing enables the precise and flexible construction of extremely complex structures that are not achievable with conventional fabrication techniques, like casting and machining. Building many objects in a single run may significantly increase productivity [24]. Because of this, 3D printing has been more popular in the scientific and technical fields since its introduction in

the 1980s. Figure 1.5 shows the typical operational steps of a 3D printing process involving vat-photopolymerization, which stands out due to its high-quality surface finishing along with high resolution. The complete 3D process includes the (A) Development of a 3D model; (B) Formulation of ceramic resin; (C) Production of the 3D printed piece using Vat-photopolymerization; then (D) Removing the solvent, which held the ceramic particles, from the printed piece and finally (E) Heating the printed piece to fuse the ceramic particles. Among the several AM processes, VAT Photo Polymerization (VPP) constitutes a polymer-based AM technology that has gained recognition. This procedure involves layer-by-layer hardening of a resin (Figure 1.5c), mostly made of monomers in a vat, on a build plate. Stereolithography (SLA), Digital Light Processing (DLP), and Continuous Liquid Interface Production (CLIP) are among the printing technologies used in VPP. A subset of VPP is SLA, a process that cures liquid photopolymer resin using a light source that is either UV or laser guided. Originally, this method was created for quick prototyping. A 3D printing (3DP) device was created by Charles Hull at 3D Systems in the early 1980s to transform liquid polymer to solid designs. Benefits of this approach include the capacity to print in several colors, the capacity to simplify complicated components printability, and the ease of printing in terms of labor and time spent. In the late 1990s, ceramic SLA was originally developed by suspending UV transparent powdered particles (at least 40% volume) in a polymer-based resin containing photo-initiators. The previously mentioned printing method is used to print this resin with a framework of support. After undergoing a heat cycle to eliminate the polymer (Figure 1.5d), these unprocessed printed parts - also referred to as "green parts" - go through a sintering stage to solidify the finished product.

As stated, structures with very complicated geometries and linked holes are hard to manufacture, since molding is typically used in these approaches. However, machining ceramic components is particularly challenging due to the material’s brittleness and hardness.

The cutting tools used are vulnerable to extreme wear, and problems, including cracking, may occur in ceramic components, making it difficult to achieve acceptable dimensional precision and surface quality [26].

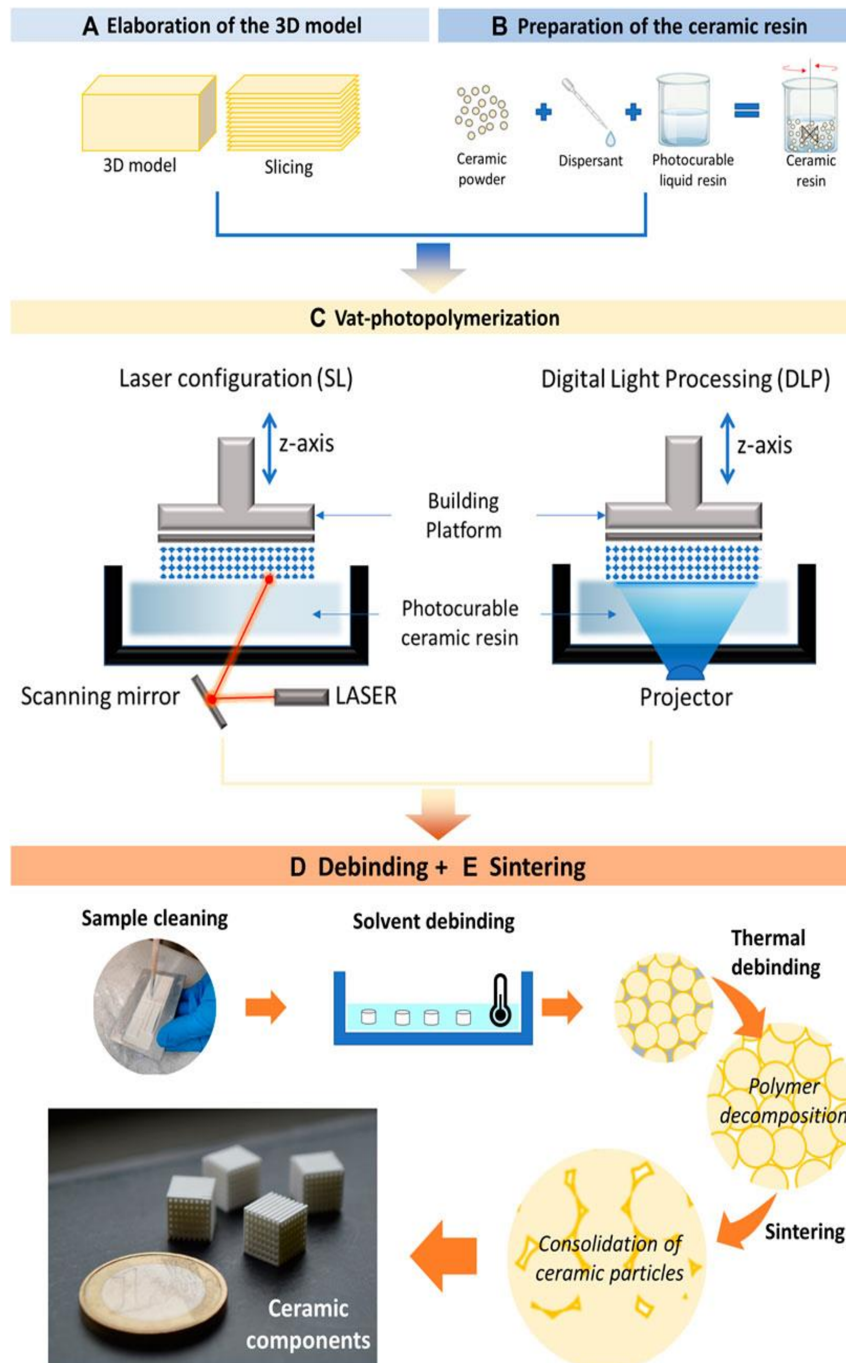

Figure 1.5. *Diagram showing the various steps to produce advanced ceramic materials via AM. The typical operational steps relate to Stereolithography (SL) & Digital Light Processing (DLP) processes [25].*

A plethora of progress has been achieved in the field of AM technology of ceramics. This research aims to explore the AM processes involved in the production of a special class of materials, specifically silver ceramic connectors, through a comprehensive investigation encompassing material properties, printing parameters, post-processing methods, and performance evaluation.

CHAPTER 2 LITERATURE REVIEW

2. Introduction

The accessibility of high-temperature materials is critical for designing new electronic and electrical power systems that can function in harsh environments. Thermal stability is necessary for viable properties at elevated temperatures, since it limits the material's breakdown of physical integrity under extreme temperatures. The recent boom in the avionic and automotive industries, oil explorations, and advanced propulsion systems require high current, high power, and elevated-temperature conditions, which created an urgent need for high-temperature materials [27, 28].

Polymers are highly susceptible to heat. Most dielectric polymers have a glass transition temperature (T_g) of less than 100°C. As the temperature rises over the glass transition temperature, amorphous polymers lose rigidity and undergo a sudden shift in physical characteristics. Thermal variations via transition temperature (T_g) for example, considerably enhance the free volume of a polymers, which is area that is not filled by molecules of the polymers, resulting in highly variable dielectric characteristics. Furthermore, because charge carriers may easily propagate throughout the material, polymer chains with a large free volume and mobility allow for significant electrical and ionic conduction [29]. Transition temperature (T_g) is often used as the primary criterion for evaluating high-temperature polymer dielectric materials, due to its impact on stability, dependability, and service life. Melting point (T_m) is also employed to assess temperature capacity in polymer materials with extremely elevated crystallinities, where crystalline phase also plays a prominent role. For achieving greater transition temperature (T_g) and melting point (T_m) values, rigid structural units are sometimes included into polymer main chains to hinder rotation and enhance stiffness. Meanwhile, existence of bulky groups is particularly useful in achieving increased

T_g and T_m values, since they physically inhibit bond rotation. Furthermore, polar side groups restrict rotation much more due to polar interactions, such as hydrogen bonding and dipole-dipole interactions, which collectively contribute to the limited freedom of rotation within polymer chains due to their stronger interactions within chain segments. Another strategy is to form intermolecular bonds that severely limit molecular mobility. Some heavily cross-linked polymers may not even undergo a glass transition [30].

Under conditions of heightened electric fields and increased temperatures, numerous polymer dielectrics demonstrate notable leakage current, wherein these materials unexpectedly conduct electricity. This phenomenon, known as emergent conduction, causes the unanticipated flow of electrical charge through the dielectric material, contrary to its intended insulating properties. Leakage current causes continual loss of energy and temperature increases in dielectric materials. This increase in temperature due to energy loss is extremely damaging in elevated temperature applications, as thermal runaway is the primary reason limiting voltage and temperature ratings [31]. For example, at 150°C, Kapton's weak-field dissipation coefficient is less than 0.1%, but with a 200 MV/m electric field, conduction loss might exceed 24%. Dissipated energy emerges as the Joule heat, which may lead the device to thermally fail. Energy dissipation is associated with a number of temperatures and field-dependent conduction processes [32]. This is why another class of materials known as advanced ceramics are being favored in terms of high temperature applicability and mechanical strength over conventional polymers.

Advanced Ceramics are the most thermally stable in the temperature range that covers the majority of the intended applications (room temperature to 350°C). These can be called high-performance ceramics, fine ceramics, engineering ceramics, high-tech ceramics, and technical ceramics. They are essentially crystalline substances with a carefully controlled composition, prepared with strict regulations using refined and described raw components

that provide specific and precise qualities. Ceramics possess a diverse array of captivating attributes as compared to other materials, such as excellent thermal insulation, low weight, a substantial specific surface area, and remarkable resistance to thermal shock. Ceramics often do not change shape over longer periods of operation, allowing for decreased maintenance costs and great stability in a wide range of organic solvents [33].

2.1. Traditional Vs Advanced Ceramics Manufacturing

Traditional ceramics components are crafted through a variety of methods, including dry forming for precise shaping without water, thixotropic casting utilizing shear thinning properties for moldability, and wet forming for intricate designs with moist clay-like materials. These techniques, alongside direct foaming, gel-casting, freeze casting, and phase inversion, offer diverse approaches to creating ceramic structures with tailored properties. Dry forming involves shaping ceramic powders into desired forms without the use of liquid binders. Techniques such as dry pressing and dry powder injection molding are examples of dry forming methods [34]. Wet forming utilizes liquid suspensions of ceramic particles to shape components through techniques like slip casting, where the ceramic slurry is poured into a mold, the liquid is then drawn out, and a solid ceramic part is left behind [35]. Gel-casting involves the use of a gel-like material as a binder for ceramic powders. The ceramic slurry containing the gel binder is poured into a mold, and the gel solidifies, forming the desired shape [36]. Thixotropic casting involves materials that exhibit thixotropy, a property where the viscosity decreases under stress and increases when the stress is removed. This property is utilized to shape ceramic materials into complex forms [37]. Direct foaming is a method where gas bubbles are introduced into a ceramic slurry to create a porous structure. This technique is often used to produce lightweight ceramic components [38]. Freeze casting involves freezing a ceramic slurry to form ice crystals, which serve as a template for the ceramic structure. After freeze-drying, the ice crystals are removed, leaving behind a porous

ceramic material [39]. Phase inversion is a process used to produce porous ceramic membranes. It involves the transformation of a homogeneous polymer solution into a porous structure through changes in temperature, solvent evaporation, or other factors [40].

Advanced ceramics are prepared by heating ceramic powders, requiring careful treatment to manage heterogeneity, particle size, particle size distribution (PSD), chemical compositions, purity, and specialized form. These parameters influence the characteristics of final ceramic components. It is conceivable to differentiate between final ceramic parts made from organically gathered materials from those made entirely using synthetic materials. A majority of binary oxide ceramics, including Al_2O_3 or SiO_2, may be produced from the non-oxide ceramics, whereas natural oxides, including elevated temperature superconductors, must be synthesized using sophisticated synthetic processes [41].

Although the market for traditional ceramic production processes is useful in terms of output, because it is confined to producing basic geometries, it is deficient in innovation as well as the customization of components, while also increasing waste [45]. Traditional ceramic manufacturing also typically requires skilled manual labor proficient in powder processing and product shaping, which could lead to material waste and elevated production expenses. Moreover, many industrial applications demand customization. Further, the traditional ceramic production process consists of numerous phases. Some of these operations, such as granulation and dewaxing, demand a lot of heat energy, which adds to the high cost and long lead time. Furthermore, it is challenging to construct complex pieces using these conventional methods, since a mold needs to be created specifically to make the parts. Occasionally, the components need to be cut from a block of ceramic pieces, resulting in labor and material waste. If the parts must be produced in large quantities, more labor hours and optimization will be needed to design and build the parts at a reduced cost of production. [42]. Figure 2.1 shows the production of high-value added products with shift to modern manufacturing

techniques. In looking at Figure 2.1, conventional ceramic manufacturing is all brought into additive manufacturing, with the production of plasma resistant parts, semiconductor parts, water filters, or joint heads as examples.

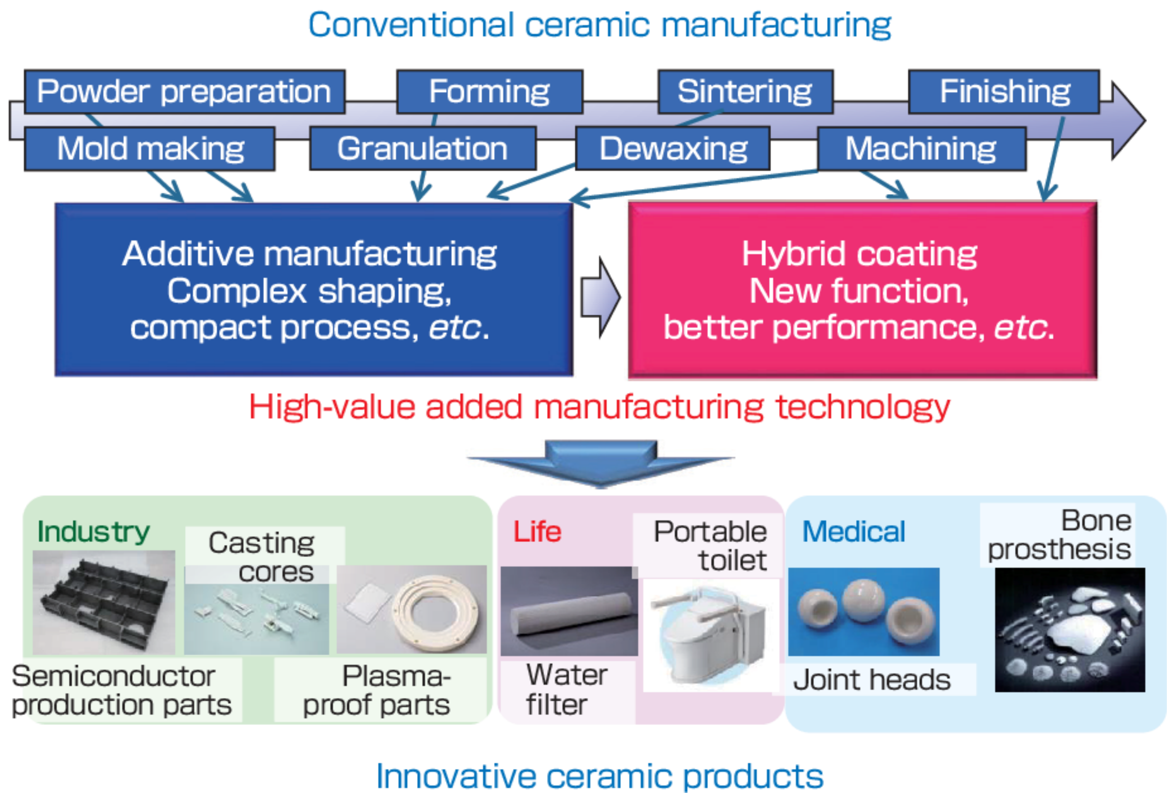

Figure 2.1. *Conventional ceramic manufacturing methods and high-value added manufacturing [43].*

AM of ceramics has emerged as an excellent choice for integrating the aforementioned various phases, since AM offers several benefits in terms of the manufacturing process and performance. AM requires no mold; therefore, components may be produced with great flexibility in a shorter time cycle and at a cheaper cost than a traditional technique. The advent of additive manufacturing enabled the production of sophisticated parts with complex shapes [42]. Figure 2.2 shows a detailed timeline of developments in the field of modern day additive manufacturing processes. It shows that since the inception of rapid prototyping in its early phases, highly processable polymeric materials have been utilised to manufacture 3D

net form parts. This progress was readily adopted in the biomedical field with majority of the innovations happening in this field. Technological advancements even enabled the processing of metallic materials, which traditionally have lesser processability compared to polymeric materials. Nevertheless, the ceramic materials, owing to their inherent qualities, have not advanced to the same extent and even in recent years AM of ceramics is in its nascent phase.

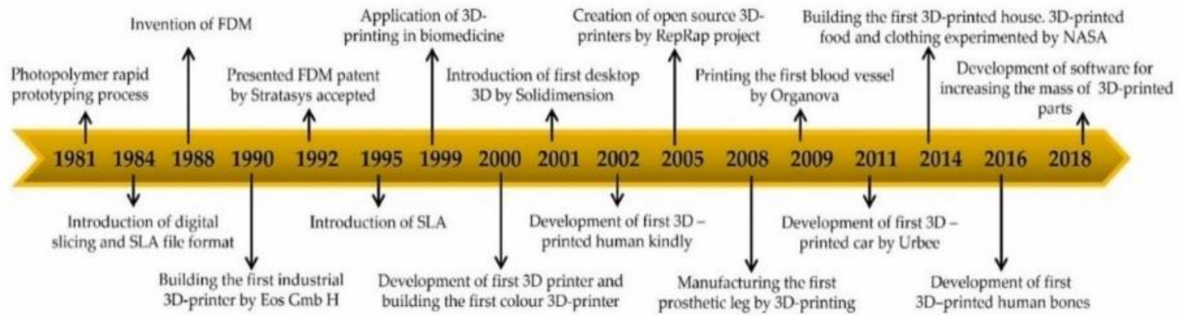

Figure 2.2. *A timeline of important developments in AM technology from 1980s to 2018 [44].*

According to the ISO standard, AM technology involves layer-by-layer fabrication of 3D objects, as opposed to formative and subtractive manufacturing. Initially, AM was mostly used to create non-functional prototypes, because of the parts' porosity and low strength features, earning it the nickname "rapid prototyping" [45].

One of the earliest groups of additive manufacturing techniques implemented for commercial purposes is Vat photopolymerization, first known as stereolithography. The production of three-dimensional parts involves the sequential application of UV energy to photocurable resin, resulting in the creation of layers as shown in Figure 2.3. The process involves (Figure 2.3A) the use of a vat or reservoir containing the liquid resin, which is selectively solidified using a light source, such as a laser or UV projector, to cure specific areas corresponding to the desired part geometry. As each layer is cured, the build platform moves incrementally, allowing for the gradual buildup of the final part. However, as depicted in Figure 2.3B overexposure, caused by light scattering, can occur in highly loaded suspensions. Recent

studies have shown the production of dense zirconia specimens without visible layer interfaces, showcasing the method's potential for intricate ceramic component fabrication (Figure 2.3B,C).

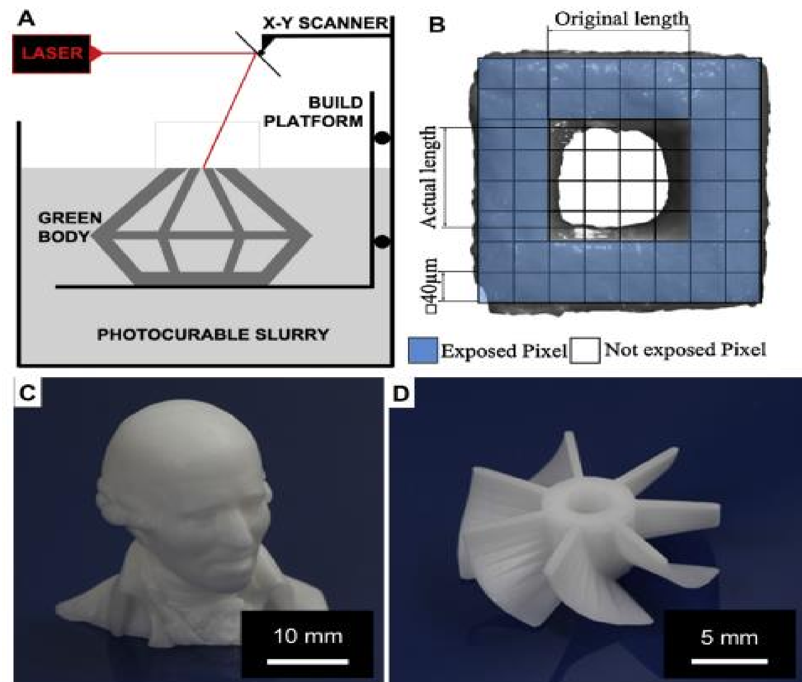

Figure 2.3. (A) *Diagram of the vat photopolymerization technology, which produces 3D components by selectively curing layer by layer a photocurable resin.* ***(B)*** *Light scattering causes overexposure in particle suspensions with large loads.* ***(C, D)*** *Post-processing resulted in dense zirconia specimens with complicated shape and no obvious layer interfaces [46]*

Recent years have seen a substantial exploration of ceramic AM as a potential solution to conventional production challenges, such as size shrinkage, complex structure construction, and excessive tool wear. The automotive, aerospace, and healthcare sectors are the main businesses that employ AM of ceramics. Moreover, 3D printing is seen to be an essential method for creating better ceramics for biomaterials and bone tissue engineering, including scaffolds for bones and teeth. For tissue engineering, 3D-printed ceramic scaffolds are more practical and expedient than more conventional methods, like casting and sintering [47].

The additive manufacturing process, which comprises a total of three steps - model generation and slicing, printing, and post-treatment, assembles materials layer by layer [44]. According to the ASTM, complicated form ceramic component fabrication utilizing AM methods is divided into two categories: direct, or single-step, and indirect process, or multi-step (see Figure 2.4). Direct procedures achieve the desired shape and final properties in one step, while indirect processes require multiple steps to achieve the desired geometry and final attributes (Figure 2.4) [44]. In the case of ceramic materials, achieving the desired characteristics requires the implementation of pyrolysis and sintering processes. These processes are essential when an indirect method is employed to shape a green body. In indirect manufacturing, initially, a mold or pattern is produced using additive techniques, which serves as a template for the final object. Subsequently, materials are cast or molded into this mold to create the desired shape. This approach is often employed for producing large or intricate objects where direct fabrication may be impractical or cost-prohibitive [44].

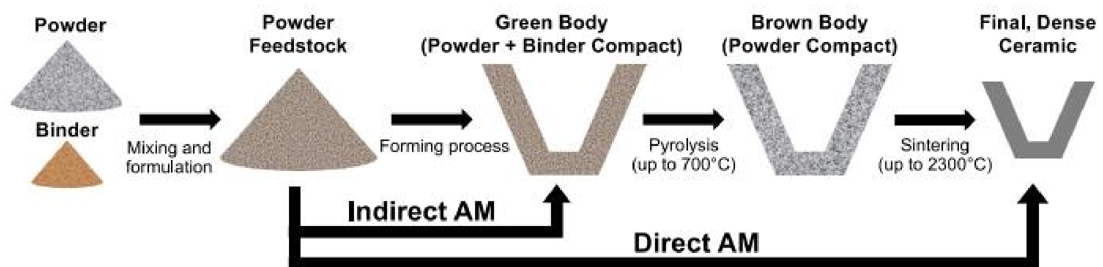

Figure 2.4 *A schematic showing the direct and indirect modes of additive manufacturing. Sintering and pyrolysis are mandatory steps when proceeded via indirect AM [44].*

Figure 2.5 shows schematic diagrams for majority of the AM techniques described here. The most widely used indirect AM technologies include sheet lamination (Laminated Object Manufacturing, LOM) [48], materials extrusion methods (MEX) (Direct Ink Writing (DIW) [49], binder jetting based methods (BJT) (two photon polymerization (TPP) [50], vat photopolymerization-based methods (VPP) (*stereolithography (SL) process)* [51], inkjet

printing (IJP) (direct inkjet printing (DIP)) [52], and indirect selective laser sintering (SLS) [53]. Currently, only two AM methods, Laser Powder Bed Fusion (L-PBF) [54] and Directed Energy Deposition (DED) [55], can build sophisticated, advanced ceramic components by shaping and solidifying material in one step.

Another AM method for processing ceramics, known as negative ceramic AM, prints sacrificial molds made of a polymer using AM techniques including Material Jetting (MJT), Fused Deposition Modeling (FDM), and Stereolithography (SLA). Here, polymer molds are then casted with a slurry of ceramic by gel casting or simple casting, which is subsequently removed via thermal burn-out or dissolution. Negative AM, or additive manufacturing, offers a superior ability to shape polymers compared to ceramics, with greater ease, efficiency, and affordability [47].

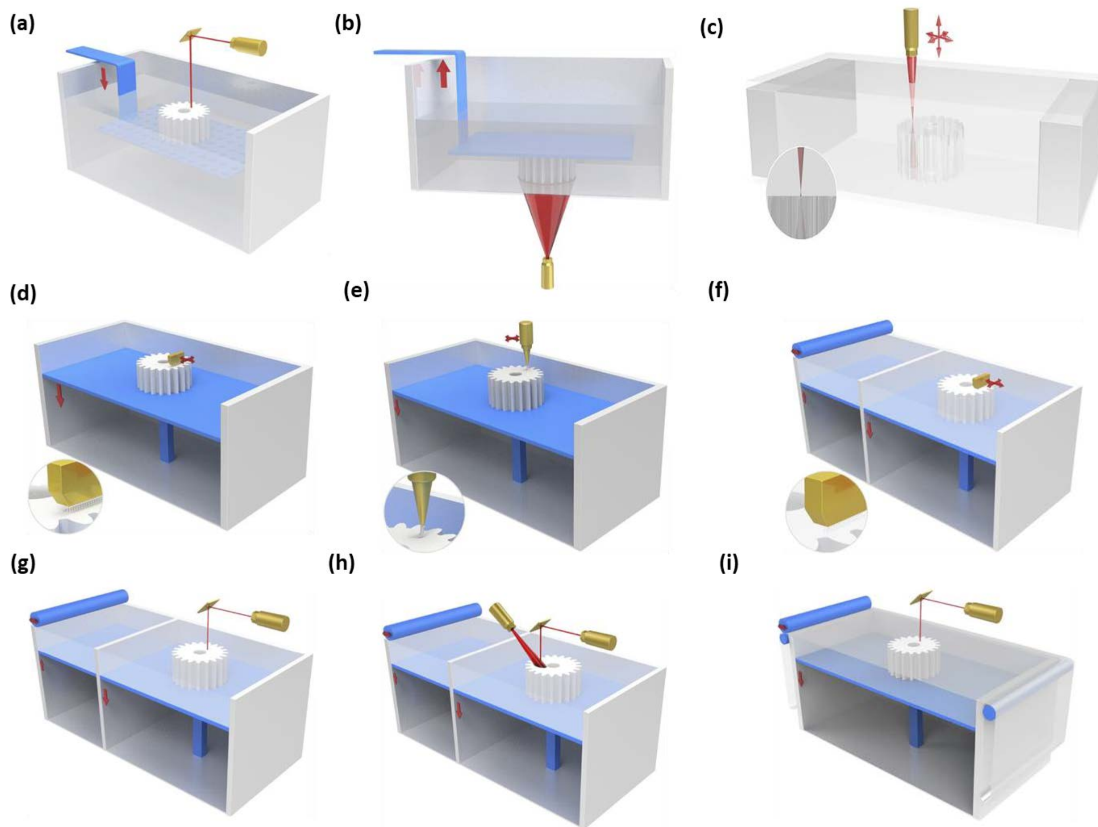

Figure 2.5. *The diagram shows the schematic representation of various AM processes.* ***(a)*** *Stereolithography (SL) process,* ***(b)*** *Digital Light Processing (DLP) process,* ***(c)*** *Two-Photon*

Polymerization (TPP) process, ***(d)*** *Inkjet Printing (IJP) process, with inset showing droplets being jetted from the printhead at higher magnification.* ***(e)*** *Direct Ink Writing (DIW) process, with inset showing a nozzle extruding ceramic feedstock.* ***(f)*** *Three-Dimensional Printing (3DP) process, with inset showing the printhead jetting a binder solution.* ***(g)*** *The SLS method.* ***(h)*** *Selective Laser Melting (SLM) and the* ***(i)*** *Laminated Object Manufacturing (LOM) process*

Expanding on the advancements in ceramic additive manufacturing, it's crucial to note the diverse array of ceramic materials effectively utilized in this process, including zirconia, silicon carbide, alumina, and silicon nitride, and polymer based ceramics. Zirconia is often produced utilizing ME-based AM, BJT, SLA, and inkjet 3D printing processes to create bespoke components, including dental items. Similarly, alumina is widely utilized as structural ceramic due to its great low cost, hardness, and heat resistance. Silicon nitride and silicon carbide have received considerable attention as highly solid materials, particularly in the aerospace sector, owing to the need to fabricate condensed products with outstanding mechanical properties [56].

2.1.1. Powder-based Deposition Techniques

Powder-based ceramic additive manufacturing involves processing each layer of a loose ceramic fragment bed as feedstock. Ceramic fragments are fused together either through powder fusion, utilizing the heat from a laser beam, or by applying liquid binders. Examples of powder-based deposition techniques include selective laser sintering (SLS), binder jetting (BJ), and laser powder bed fusion (L-PBF). Powder bed fusion can occur in either a single phase or multiple stages, depending on the selective fusion of powder particles in the bed. [57]. In a single-phase fusion process, the fusion of the powder particles occurs in a single step or stage. This means that all the necessary conditions for fusion, such as heat or binder application, are applied simultaneously, or in a uniform manner, across the entire powder bed. Conversely, in a multiple stage fusion process, the fusion of powder particles occurs in

several distinct steps or stages. This could involve applying heat or binder selectively to specific areas of the powder bed, rather than uniformly across the entire layer. Depending on the particle size, the thickness of the powder layer will vary from 20 to 200 µm. Four types of fusion processes, or binding mechanisms, are distinguished: liquid-phase sintering (partial melting), solid-state sintering, chemically induced binding, and full-state melting [58]. In liquid phase sintering, partial melting of powder particles forms a liquid phase, which acts as a binder upon solidification, promoting strong bonding between particles. In solid-state sintering, powder particles are heated below their melting point, inducing atomic diffusion and solid-state bonding between adjacent particles, leading to consolidation. Meanwhile in the chemically induced binding, chemical agents or binders react with powder particles to form bonds, either during or after deposition, providing control over the bonding process. In full-state melting, powder particles are heated to their melting point, fully liquefying and merging into a homogeneous liquid pool, which solidifies upon cooling to form the final part.

SLS is one of the important powder deposition techniques. The method of SLS was developed in the 1980s to produce polymeric structures with near-net shape. It entails utilizing a CO_2 laser to fuse, or sinter, powdered substance. Using a roller, the powder is added to build chamber's surface. Once powder particles have been evenly dispersed in a bed, the particles are just heated to below their melting point to create the designed part, using cross sectional slices from a virtual CAD model for each layer. A broad spectrum of inexpensive, green materials may be produced fully dense, extremely precise components [59].

Another powder-based deposition method is laser powder bed fusion (L-PBF) used to make complicated form ceramic components. This technology, like SLS, uses high-energy laser sources. L-PBF is a time-saving technique, which produces components by entirely melting powders by employing laser sources of greater energy density and requiring no binder or

post-sintering step for additional processing, as compared to SLS. The L-PBF technique is widely regarded as the one and only 3-D printing method that produces readily available, complex ceramics having better purity, a very low porosity, and higher strength, while employing single step and in a short amount of time. Although ceramics produced using L-PBF exhibit promising potential, the process is more complicated compared to metallic materials due to inherent issues, such as porosity, rough surface finishes, low dimensional accuracy, and inadequate densification of final product. As a result, the applications of L-PBF ceramics still remain restricted.

Ceramics produced via L-PBF show weak thermal shock resistivity; therefore, fractures, as well as distortions, arise in due to thermal stress [60]. Shishkovsky et al. used the L-PBF method on ZrO_2 components and discovered fractures and wide open holes in the finished parts [61]. Mercelis et al. investigated the impetus of residual stresses in the L-PBF-manufactured goods [62]. The researchers devised a pristine theoretical model to understand the presence of residual stresses. They too discovered the scanning approach of the laser in L-PBF has a significant impact on the degree of residual stress. Moreover, maintaining consistent quality during printing became challenging, due to partial melting caused by the short contact time of the laser while scanning, resulting in inferior surface quality. Gan et al. utilized the L-PBF technique to manufacture spodumene glass-ceramic [63]. The spodumene-Al_2O_3 samples were produced with increasing layer thickness. Figures 7a-c show MicroCT images of samples produced at a temperature of 950 °C, with different layer thicknesses. It is evident that the size of the pores decreased as the thickness of the layer increased. Smaller pores indicate a denser microstructure, enhancing structural integrity and improving mechanical properties like strength and toughness. Additionally, smaller pores result in a smoother surface finish, reducing surface roughness and enhancing aesthetics and functional performance, particularly in applications requiring low friction. Moreover, minimizing pore

size reduces the likelihood of defects such as cracks or voids forming within the material, thereby improving overall part quality and reliability. In L-PBF, where layers of material are melted and fused together, controlling pore size is essential for achieving high-quality parts.

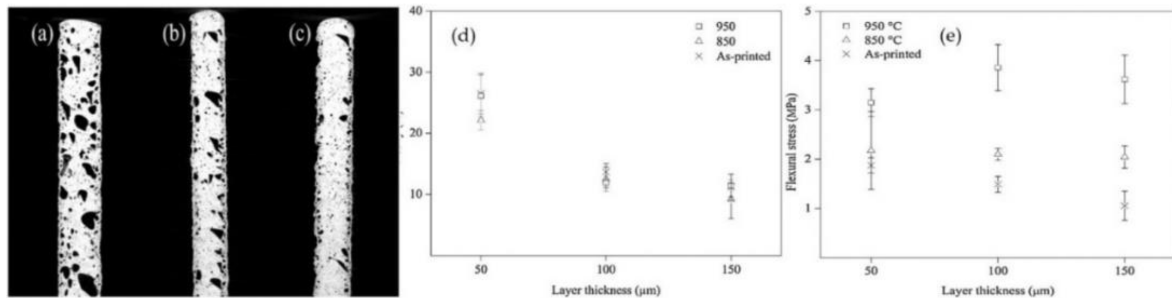

Figure 2.6. (a) ***(a)*** *MicroCT image of 3 samples* ***(d)*** *percentage of porosity,* ***(e)*** *the flexural strength of the L-PBF-printed spodumene-Al_2O_3 samples at various temperatures [93].*

BJT is known as an indirect 3D-printing technique that is defined as an "AM process in which a liquid bonding agent is selectively deposited to join powder materials" [64]. Powder roller distributes a very thin coating onto the construction platform to create a bed. Printer then administers a dropwise solution of an organic binder to CAD-defined portions of the surface of the bed. The binder facilitates adhesion of powder particles in the designated locations. The first layer could be constructed like this, and then platform could be lowered by a known height, and fresh layer is distributed on previous one [65, 66]; this continues util the desired part is completed.

Alumina was among the first ceramics studied by binder jetting [67]. Manotham et al. investigated porosity, density, the capacity of shrinking and micro-structures with the physical characteristics and print designs of alumina [68]. The printed sample showed 11% of shrinkage, 39% of density, 1.04 MPa of flexural strength, and 1.78 MPa of compressive strength. Gaytan et al. employed the BJT technique to create barium titanate (BTO). Sintered samples had densities of 41.4%, 60.6%, & 65.2% at 1260 °C, 1330 °C, and 1400 °C. Figure

2.7 shows the powder aggregated together, without fully fusing at 1260°C (a & b). At 1330°C (c & d), grains grew unevenly, with spaces between the grains and irregular pores. At 1400°C (e & f), grains grew uniformly and porosity was reduced. Because of their piezoelectric capabilities, the BTO samples would be good candidates for sensor applications in gas turbines, power plants, and oxy-fuel combustion [69].

The laser-based directed energy deposition (DED) method, also called Laser Energy Net Shaping (LENS), Laser Cladding (LC), or Laser Metal Deposition (LMD), was initially employed in the mid-1990s [70]. In DED, feedstock materials are laid into a molten pool created by a heat source [70]. The DED technique employs a laser beam of high power to melt ceramics with melting points of close to 3000 °C. This approach has been used to create ceramic oxide components including alumina, zirconia, mullite ceramics, alumina ceramics, and zirconia-alumina ceramics.

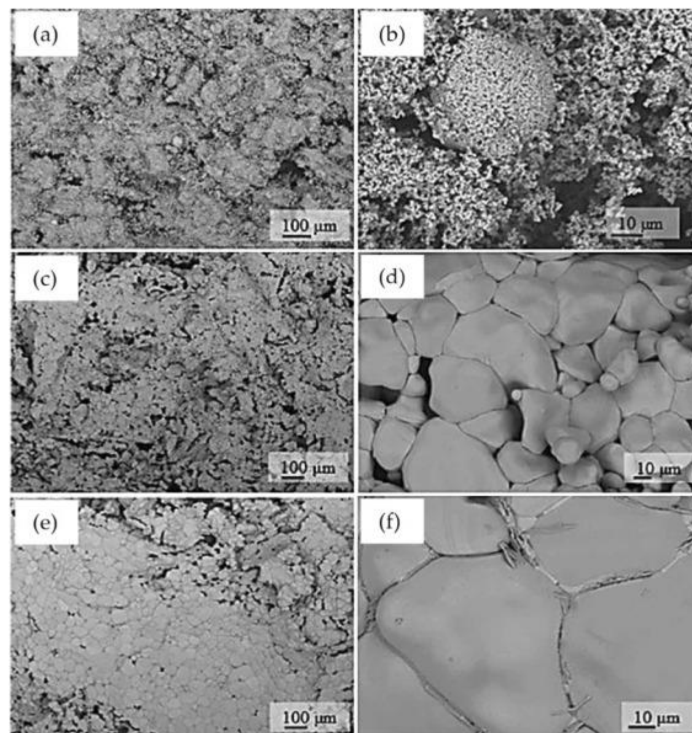

Figure 2.7. *SEM images related to barium titanate after being sintered at (a & b) 1260 °C, (c and d) 1330 °C, (e and f) 1400 °C for 4 hours [113].*

2.1.2. Bulk-Solid Based Deposition Techniques

Sheet lamination (SHL) uses thin sheets of solid material to construct items utilizing additive, as well as subtractive processes. Such layers are joined by applying heat with pressure to create a thermal adhesive covering. Griffin et al. originally published the SHL approach for ceramic manufacture in 1994, using tape casting of Al_2O_3 with ZrO_2 green sheets etc. Other structural ceramics include glass-ceramic composite, Si/silicon carbide composite, silicon carbide, titanium carbide/nickel composite, zirconia and alumina/zirconia composite, and functional ceramics [71].

Material Extrusion (MEX) is another bulk-solid based deposition technique in which ceramics in paste form are extruded through a nozzle and deposited to create a three dimensional structure. This technique uses a variety of technologies to form advanced ceramics, including wax-based and water-based extrusion related processes [72]. One of the primary advantages of MEX is its simplicity and affordability compared to other additive manufacturing methods. Desktop 3D printers utilizing MEX technology have become increasingly accessible to hobbyists, educators, and small businesses, enabling rapid prototyping and customization of objects.

Another bulk-solid based deposition technique is fused deposition modeling (FDM). Crump et al. pioneered FDM, which is now considered as the most famous AM process [73]. This approach utilizes cost-effective and eco-friendly raw materials, which can be classified into two categories: non-fused and fused materials. In non-fused materials, including concrete and ceramics, the condition of the materials remains constant throughout the operation, and flow of viscous paste is accomplished by atmospheric pressure. Some print heads in this technique enable the co-printing of support related structures for samples with complicated geometry, as well as the printing of samples with numerous materials. Furthermore, the FDM method

can print multicolored items from various materials without merging them together. However, because of the filament thickness, printed pieces have poor surface quality; thus, polishing the created objects is required to get a smoother surface. FDM has several applications, including drug delivery, sensors and shielding, quick tooling, fashion, architecture, automotive, microfluidics, education, aerospace, prosthetics, 4D printing. For fused materials, the condition of the components undergoes a transition from solid to a thick paste while reverting back to solid. The solid undergo a phase transition and transform into a thick and sticky substance by the application of heat. Subsequently, it is expelled out the nozzle using a numerically controlled process. Figure 2.8 shows SEM images of a ZrO_2 (BCP/ZrO_2 scaffold), which was made using FDM process for the purpose of bone tissue engineering. The mechanical tests conducted on the scaffolds revealed that the compressive strength rose from 0.1 MPa to 0.5 MPa when comparing pure BCP with BCP containing 10 wt% zirconia. The inclusion of ZrO_2 powders was discovered to significantly bolster the mechanical properties of prepared biphasic calcium phosphate scaffold.

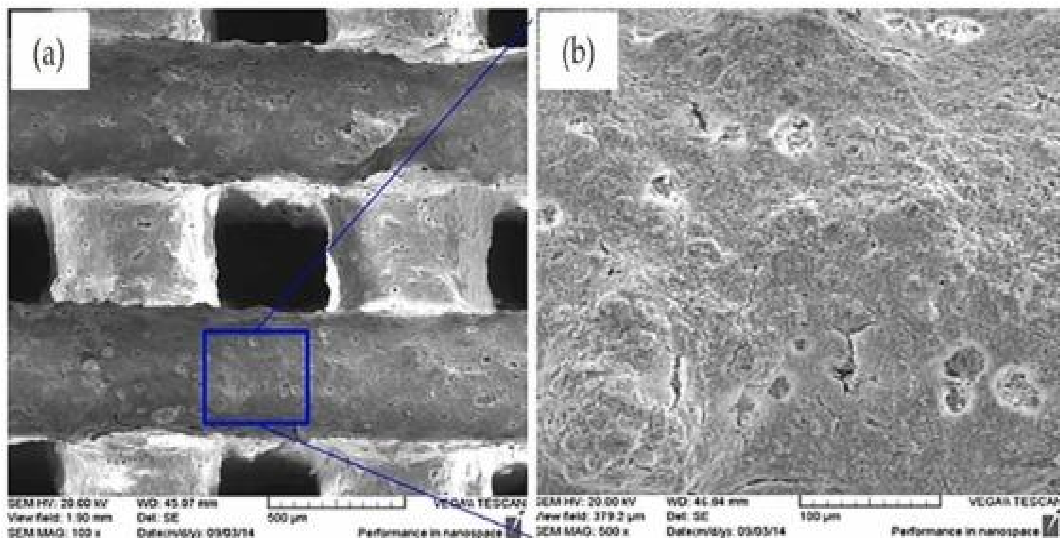

Figure 2.8. *BCP/ZrO_2 scaffold SEM images:* **(a)** *approximately 350 µm pore size as well as 500 µm printed lattice breadth;* **(b)** *granular interface of the FDM-manufactured structure following printing along with sintering [210].*

2.1.3. Slurry-Based Deposition Techniques

AM of slurry-based ceramics typically involves dispersing ceramic ingredients as feedstock, such as inks and pastes, depending on the viscosity and solid loading of the system. The slurry could be printed employing inkjet printing or photopolymerization with the addition of extrusion method.

Material jetting (MJT) is a 3D-printing method that employs inkjet technology delivered by hundreds of micro-sized nozzles. The droplets of the constructed material are deposited selectively, resulting in filament-like formations [74, 75]. In this technology, raising the inclination of surface of the area of printing reduces the roughness of the surface, which has not been observed in other AM techniques [76].

Vat photopolymerization (VPP) is a common AM technology for producing ceramic materials that use inks with photo-curable properties during the printing process [51]. This technique has received the majority of attention in academic as well as industrial domains because of its advantages, which include high speed, perfect dimensional precision, and a wide variety of applications in the biomedical applications, functional devices, and ceramics. The VPP procedure involves suspending ceramic powder in a monomer or oligomer doped with the photo-initiator. The solution is then exposed to a UV6 lamp UV light, causing polymerization. The green body then undergoes de-binding and sintering at elevated temperatures to produce the final ceramic [77].

Stereolithography (SLA) technology was the first ever commercially viable solution released to market because of its high levels of precision, clean finish, and strong chemical bonding among the layers [78]. The technique is based on "top-down" approach, where it may produce many tiny samples at the same time since prepared specimens are orientated close to one another on the same construction platform. Halloran et al. have extensively explored

SLA approach since 1994, beginning with use of extremely dense ceramic samples up to 65 vol%, such as alumina, silica, and silicon nitride [78].

Heating and cooling are crucial stages in numerous AM methods. Figure 2.9 presents a comparison of the speed of production, resolution reached, and specific energy required in seven primary additive manufacturing (AM) techniques. AM primarily relies on electromagnetic radiation for energy transfer between the laser head and the material. Additionally, heating and cooling play significant roles in many AM methods. For instance, Binder Jetting employs binders that need lower heat levels, but choosing durable and suitable binders is vital. AM involves non-equilibrium solidification, emphasizing the importance of material sustainability under varying conditions. For ceramic parts, hot and cold working, heat treatment, and surface finish are critical for load-bearing and repetitive cycle applications.

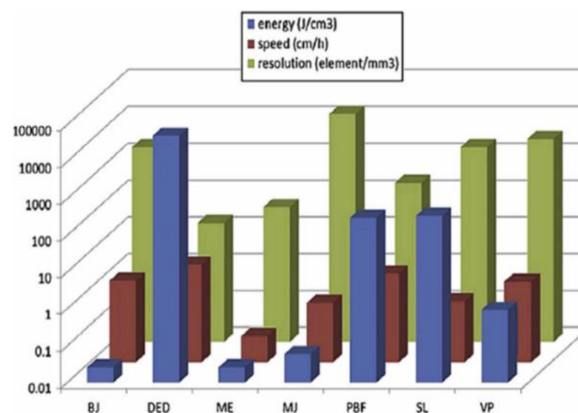

Figure 2.9. Comparing the relative energy applied, speed of the additive manufacturing process, and resolution of created items utilizing seven primary types of additive manufacturing processes [41].

Over the last few decades, research has focused on the development of ceramics with a wide range of applications, including energy transformation, biomedical applications, transportation systems, storage materials, anti-frosting, wastewater and water treatment, pervaporation, antifogging, information technology, anti-corrosive applications, and

manufacturing technology [79]. Furthermore, ceramic components have shown to be highly attractive in a multitude of electronic appliances, including integrated circuits, automotive, telecommunication, isolators, filters, circulators, di-electric resonator antennas in microwave, phase shifters, millimeter wave communication, and different radar systems, because they can be operated at the elevated temperatures, in harsh environments, and at high frequencies with power [79].

Ceramic materials, like borides, oxides, carbides, and nitrides, are being used to create customized microstructures and properties (including hole/electron carrier mobility) for applications in electronics [42]. Structural ceramics for elevated temperature applications have emerged as a promising study field. These ceramics must have features like resistance to creep deformation at the interfaces, low volatility, thermal shock resistance, oxidation resistance, and adequate solidity at normal temperature to meet the stringent demands of their intended applications [80].

Some of the non-oxide ceramic components constructed of Si_3N_4 and SiC show promise for high-temperature applications, but are less likely to function over 1500 ^oC [79] . Silicon-based ceramics have demonstrated considerable potential in the next-generation of gas turbine engines [81]. However, they degrade rapidly in an H_2O vapor environment owing to volatilization of protective SiO_2 scale.

The packaging offers electrical connectivity to the external world, protects the semiconductor chip from dangerous chemicals, and also allows for chip manipulation. The majority of ceramic parts employed in microelectronic packages are made of alumina, glass ceramic, zirconia, beryllia, or magnesia. Alumina has a high dielectric strength and offers effective electrical insulation, while the high thermal conductivity of copper creates a good heat sink. However, alumina is not a suitable material for certain microelectronic packaging

applications due to its greater coefficient of thermal expansion (CTE) as compared to silicon, low thermal conductivity, and high relative permittivity (dielectric constant), all of which can cause a high frequency signal drop [82]. Ceramics with high potential to replace alumina, such as aluminum nitride, have been actively researched as prospective replacements for component materials [82]. Use of the alternative components necessitates the development of a strong and appropriate joining method to connect the ceramic parts to the heat sink material.

2.2. Ceramic Metal Connectors

There are still many vital technologies that need to be developed, such as methods for joining and sealing metals to ceramics. Currently, polymers are mostly used as a sealing material for electrical penetration; however, polymers have a limited working life, weak air tightness, and poor resistance to radiation and elevated temperatures [83]. The molecular structure of polymers is also susceptible to thermal degradation, leading to diminished mechanical strength, increased brittleness, and potential failure under extreme thermal conditions [84] . Such limitations hinder the viability of polymers in applications requiring sustained performance at elevated temperatures, thereby necessitating alternative materials solutions.

As a result, ceramic-metal sealing and connecting technology has become increasingly crucial. The usage of ceramics in the form of structural material has expanded potential applications [85]. For example, when first space station was created, metal and ceramic connections were critical to its construction and functioning [86] . Ceramic and metal connections were also employed in these nuclear and solar devices to convert the produced energy from those methods to electricity [87].

Similarly, a ceramic coating could be employed to give necessary firing frequency for controlling the right temperature within the space station construction. Spacecraft

performance is frequently dependent on the strength supplied by ceramic-metal connections, corrosion resistance, and the capacity to withstand high temperatures [88, 89].

The main methods to realize permanent sealing between metal parts and ceramic components are gradient powder connection [90], hot pressing connection, air pressure connection, active metal brazing [91], electron beam welding, glass solder [92], ceramic brazing [93], *in situ* ceramic sintering [94], and *in situ* glass crystallization.

2.3. High Temperature Co-fired Ceramics & Low Temperature Co-fired Ceramic

Modern electronic equipment are currently being constructed using integrated circuits, which are made up of linked parts (transistors, resistors, etc.) stored on a small silicon chip. This circuit is then put together on packages with substrates that provide insulation [95]. The substrate's foundation is then used to make electrical connections to the tiny electronic parts [95]. High Temperature Co-fired Ceramic (HTCC) and Low Temperature Co-fired Ceramic (LTCC) are two distinct ceramic substrate technologies widely utilized in electronic packaging. HTCC involves the fabrication of ceramic substrates through the co-firing of multiple layers of ceramic tapes or green sheets at temperatures nearing 1600°C [96, 97]. This process integrates conductive traces and electronic components into the ceramic layers, resulting in substrates known for their exceptional thermal conductivity, mechanical strength, and reliability in high-temperature environments, making them suitable for demanding applications [98, 99]. Table 2.1 shows a detailed listing of chemical as well as physical properties of HTCC components [99]. The table compares the properties of three ceramic materials: Alumina (Al_2O_3), Aluminum Nitride (AlN), and Zirconium Silicate ($ZrSiO_4$). It includes a range of properties such as dielectric constant, thermal conductivity, and flexural strength. For instance, AlN stands out with high thermal conductivity (200-230 W/m K), making it suitable for applications where heat dissipation is crucial. On the other hand, LTCC

technology enables the co-firing of ceramic layers at lower temperatures, typically between 850°C to 900°C. Figure 2.10 shows the LTCC circuit board production cycle. It involves the layering of ceramic dielectric sheets produced through tape casting. Using screen-printing techniques, conductive patterns, resistors, or capacitors are applied onto these sheets. The assorted tapes are then combined and pressed together to form multilayer circuits. Subsequently, holes are metallized via the layers, referred to as vias, facilitating connections between among various conductive patterns. Following lamination, green stack is subjected to treatment by heat to remove organic materials and increase component density [99].

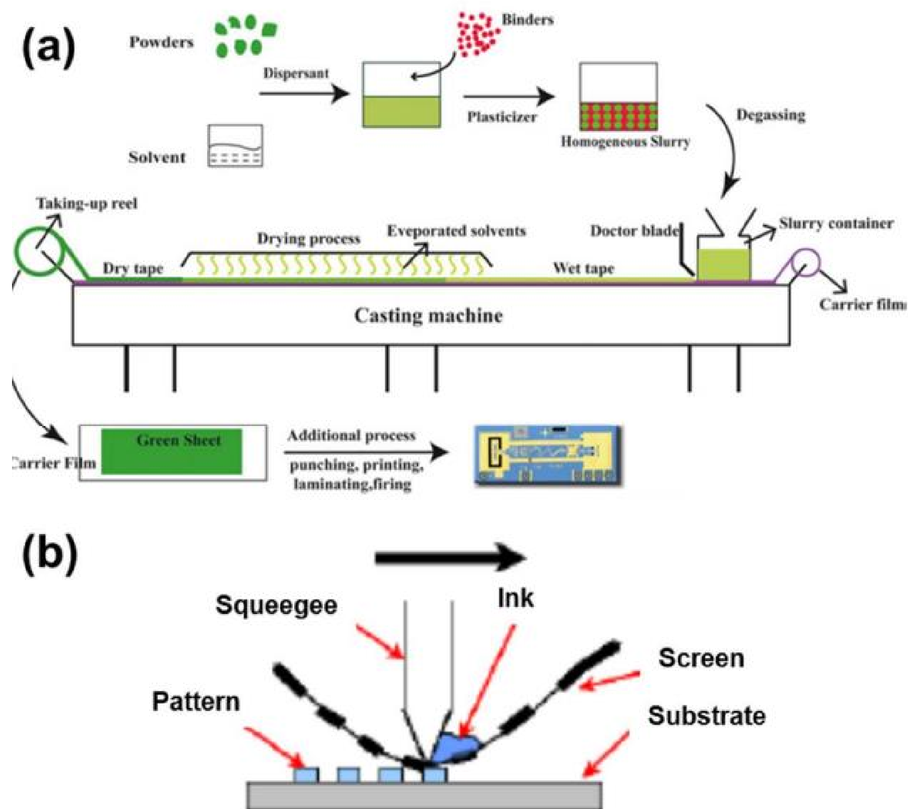

Figure 2.10. LTCC circuit board production cycle [99].

LTCC substrates, fabricated using ceramic tapes with dispersed particles and binders, allow for the integration of not only conductive traces but also passive components like resistors and capacitors within the ceramic layers. LTCC finds extensive use in radiofrequency (RF)

and microwave applications due to its excellent electrical properties, low signal loss, and high-frequency capabilities [100]. Both HTCC and LTCC offer unique advantages tailored to specific electronic requirements, from high-power applications to RF circuitry, contributing significantly to the advancement of electronic systems and miniaturization.

Additive manufacturing (AM) enables the automation of production processes, facilitating the creation of intricate 3D metallic circuits beyond conventional methods. It also allows for the production of complex ceramic packing shapes and the reduction of individual layer thickness in the manufacture of HTCC or LTCC components. By depositing the required material at each voxel during creation, AM technologies offer the flexibility to access specialized designs for enhanced attributes or novel functionalities. Moreover, AM minimizes raw material wastage and eliminates the necessity for tools, thereby potentially reducing production costs [99, 101].

Table 2.1. Chemical as well as physical properties of HTCC components [99].

Properties	Alumina	AlN	$ZrSiO_4$
ε_r	9.5–9.9 (10 GHz)	8.0–9.2 (1 MHz)	9.2 (5 GHz)
tan δ	0.0001–0.0004 (10 GHz)	0.001 (1 MHz)	0.0003 (5 GHz)
Density (gm/cm^3)	3.8–3.95	3.25–3.3	4.2–4.3
Thermal conductivity (W/m K)	25–35	200–230	15
Poisson's ratio	0.2 to 0.23	0.25	
CTE (ppm/°C)	6–8	4.2–5.8	–2.5
Flexural strength MPa	450–650	300–450	150–200
Hardness Moh's	9.0	7.0	6.5–7.5
Volume resistivity RT	1×10^{14}	$>10^{13}$	–
Dielectric breakdown voltage	>15 KV/mm	>15 KV/mm	–
Water absorption	Nil	Nil	Nil
Color	White	White/gray	White
Sintering temperature (°C)	1500–1700	1700–1900	1600

Substrate-based components using HTCC and LTCC span a broad variety of applications. Examples include lab-on-chip systems, intelligent 3D packages, like Si-chip packaging,

electronic components including multilayer actuators, multilayer capacitors, resistor-capacitor filters, and 3D multichip modules, including for use in gearbox controls, engineering management platforms, automotive applications, and high-frequency applications in aerospace and medical engineering [102].

2.4. Research Problem Statement

This research endeavor is related to the fabrication of high temperature silver ceramic connectors. The traditional methods employed for preparing metal ceramic connectors often encounter significant challenges related to the formation of poorly integrated ceramic-metal interfaces [103] . These conventional techniques, which typically involve processes such as hot pressing, often result in suboptimal structuring, leading to exposed metal regions susceptible to thermal degradation and mechanical failure [8]. The inadequacies inherent in traditional methods underscore the pressing need for the adoption of additive manufacturing techniques as a superior alternative for fabricating high-temperature silver ceramic connectors.

The deficiencies observed in traditional manufacturing processes stem from their inherent limitations in achieving precise control over the deposition and distribution of materials at the microstructural level [8] . During sintering or hot pressing, the fusion of ceramic powders and metal components occurs under high temperatures and pressures, often leading to non-uniform distribution of phases and incomplete interfacial bonding [104]. Consequently, the resulting ceramic-metal interfaces may exhibit irregularities, voids, or discontinuities, thereby compromising the structural integrity and thermal/conductivity performance of the composite material [104]. In contrast, additive manufacturing offers a paradigm shift in materials fabrication by enabling layer-by-layer deposition of materials with unprecedented precision and control. Additive manufacturing facilitates the creation of complex geometries and

tailored microstructures with minimal waste and enhanced reproducibility.

The utilization of additive manufacturing for fabricating silver-based ceramic connectors mitigates the shortcomings associated with traditional methods by offering several distinct advantages. Firstly, additive manufacturing enables the production of intricate geometries and customized designs that are impractical or impossible to achieve using conventional techniques [105]. This flexibility in design allows for the optimization of thermal conductivity, electrical connectivity, and mechanical strength, thereby enhancing the overall performance of the connectors under high-temperature conditions. Secondly, additive manufacturing facilitates the integration of metal components within ceramic matrices with precise spatial control and homogenous dispersion, minimizing the occurrence of interface irregularities [106] .

Ceramic surface roughness also poses a significant concern in the performance and reliability of metal ceramic connectors, particularly in high-temperature environments. Irregularities or rough patches on the ceramic surface can impede the uniform distribution of the metal phase and compromise the integrity of the interface between the ceramic and metal components. This may lead to increased contact resistance, thermal stress concentration, and susceptibility to mechanical failure under thermal cycling conditions [107]. This research aims to minimize ceramic surface roughness and enhance the interfacial bonding to enhance the functionality of metal ceramic connectors.

The flow of electrons within the metal phase of silver ceramic connectors represents a critical aspect of their electrical conductivity and performance. Traditional connector designs may exhibit limitations in facilitating efficient electron flow due to factors such as grain boundary scattering, impurities, or discontinuities within the metal microstructure [108]. These impediments to electron mobility can result in increased electrical resistance, energy losses,

and degradation of electrical performance over time.

This research was conducted to develop a novel approach for applying a uniform, smooth layer of metal to ceramic substrates, particularly focusing on reducing surface roughness. In this pursuit, the efficacy of utilizing silver paste deposition was explored, as a method intended to mitigate the challenges associated with rough surfaces commonly encountered in traditional connector fabrication methods. Thus, to address challenges of high-tech connectors, novel silver ceramic based connectors were explored that could optimize electron transport pathways within the metal phase and create a smoother surface silver deposition, thereby enhancing the conductivity and reliability of connectors.

CHAPTER 3 METHODOLOGY

3. Introduction

This chapter explains the approach employed to fabricate and evaluate high-temperature ceramic silver connectors for advanced electronic applications. It describes the procedures involved in the manufacturing of ceramic substrates, from the selection and formulation of raw materials to the precise execution of 3D printing, curing, and sintering processes. The methodology also encompasses the deposition of silver conductive designs onto ceramic substrates, utilizing cutting-edge printing technologies and specialized conductive pastes. Moreover, this chapter provides the comprehensive characterization methods employed to assess the electrical conductivity, adhesion strength, and microstructural integrity of the printed silver connectors.

3.1. Materials

Amorphous fused silica (SiO_2) ceramic photopolymer resin was purchased from Formlabs, Inc., (Somerville, MA, USA). Silver Conductive Paste was purchased from ACI materials Inc.

3.2. Equipment & Software

Voltera V-one 100-120V, 4.7A (SN-V1-07-2176-120), purchased from Voltera, Inc. was used to print the silver paste onto the ceramic substrate.

Multimeter (U2130) series 3.5, purchased from Keysight Technologies was used for conductance measurements.

Keyence VHX-7100 digital microscope (5E120024), purchased from Keyence Corporation, Japan was used for microscopic analysis of fabricated connectors.

The Formlabs Form 2 SLA 3D printing machine (Formlabs, Inc.) was used to print the ceramic substrate.

Instron® Universal Testing Machine, 3400 series (500N to 300kN) was used for peel testing.

Debinding Sintering Furnace (480V) 450-CH-180, purchased from Admatec Additive Manufacturing Technologies (Hamsterkoog 7, 1822 CD Alkmaar, Netherlands) was used for sintering purposes.

Benchtop Muffle Furnace (4800), purchased from Thermolyne (LLC) was used for curing silver paste.

Digital caliper (LF04) (150 mm/6 inch), purchased from Deqing Liangfeng Electronic & Technology Co. Ltd was used for thickness measurements.

3.3. Manufacturing of Silver Ceramic Connectors

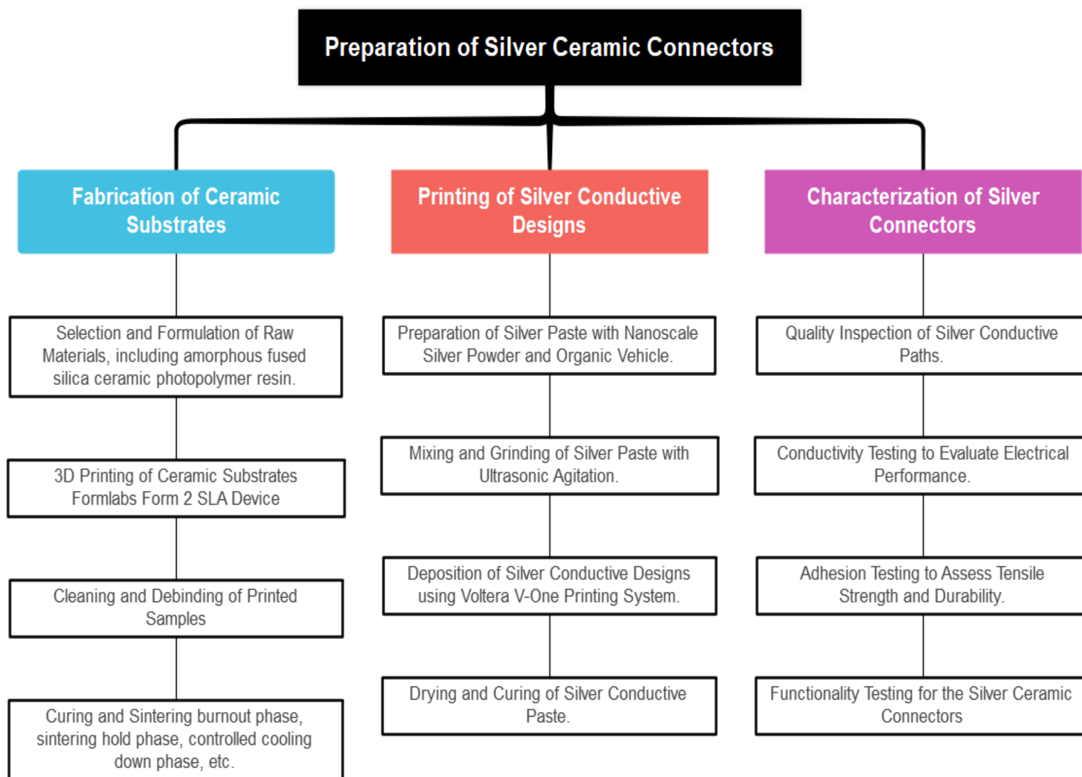

Figure 3.1. *Flow diagram showing the 3 distinct processes for the fabrication of silver*

ceramic connectors and their characterization by various techniques.

The procedure to fabricate silver ceramic connectors could be divided into 2 main stages: the manufacturing of ceramic substrates and the printing of silver conductive designs. Figure 3.1 illustrates the detailed steps taken for both of these stages. The main procedure for ceramic fabrication involved selection of material and printing in the form of ceramic proceeding with debinding and subsequent sintering process. The steps for printing of silver conductive designs include agitation and deposition of silver paste over ceramic substrate with subsequent curing of printed silver paste

3.3.1. Printing of Ceramic Substrates

The parts in this study were made using readily accessible amorphous fused silica (SiO_2) ceramic photopolymer resin from Formlabs, Inc. (Somerville, MA, USA). Using an Abbe Mark II refractometer and an L3 spindle, a Fungilab viscometer was used to measure the resin's viscosity along with refractive index. A Formlabs Form 2 SLA device featuring a 405 nm laser light source and some 50-micron layer thickness was used for the printing procedure. Standard Tessellation Language (*.stl) files created on CAD software (SolidWorks), which were sliced by Formlabs Software, were used to print the resin. The pre-form program divides the *.stl files to layers based on user-specified resolution, resin type, layer thickness, and point density. The program attached a support system to the substrate samples such that the CAD model was constructed upside-down. The models have support systems set up on a 14.5 cm by 14.5 cm construction platform, which can hold building components that were 17.5 cm high. A resin tank holds the resin that comes from a cartridge and travels in accordance with the *.stl model. The build platform moves up vertically in accordance with the height of 3D model. Here, top-down printing was used to print samples at a temperature of 35°C in the flat XY plane along with vertical Z orientations. The printing process used a 405 nm wavelength, 50 µm layer thickness, and 140

microns of laser spot resolution. The samples were printed using a support system oriented at 90 degrees, which is the ideal angle to print flat components. After removing the printed samples from the build plate, they were given a minimum of 15 minutes to be cleaned with isopropyl alcohol (IPA) to eliminate any remaining resin. After being cleaned in IPA, the samples were subsequently air dried and debonded in air at 400°C. At this point, the ceramic samples in the constructed geometry are left behind when the resin in the ceramic SLA samples evaporates.

3.3.2. Sintering

The next step involved the sintering process of green parts obtained (see Figure 3.2). The sintering parameters are detailed in Table 3.1, while Figure 3.3 shows temperature profiling of sintering process in graphical form. In the conducted study, the sintering process was initiated with a gradual increase in temperature during Ramp 1, which reached 240°C over a span of 240 minutes. This slow heating method effectively removed any moisture or volatile substances present in the material, thereby preventing sudden thermal shocks that could have compromised the sample's integrity. Following Ramp 1, the Burnout phase was implemented to eliminate organic components and residual binders from the sample. This phase involved heating the material to 300°C over 60 minutes and then keeping the samples at 300ºC for 720 minutes. The extended duration ensured thorough removal of organic substances, minimizing the risk of undesirable reactions or contamination during subsequent sintering stages.

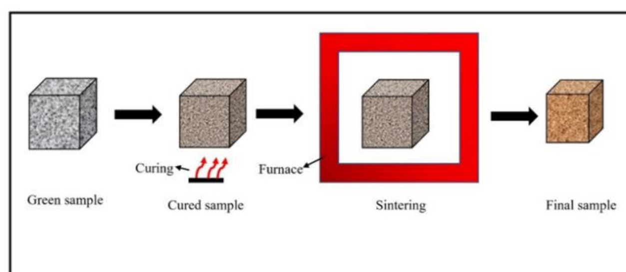

Figure 3.2. *Diagram showing the sintering process.*

Transitioning from the Burnout phase, Ramp 2 facilitated the increase in temperature to the desired sintering temperature of 1271°C over 1173 minutes. This controlled temperature ramp allowed for gradual densification of the material, minimizing the risk of thermal stresses and cracking while promoting particle rearrangement and compaction. Following Ramp 2, the material was subjected to a Sintering Hold phase, during which it was maintained at 1271°C for 5 minutes. This duration was optimized to balance densification kinetics and minimize excessive grain growth, ensuring the desired microstructure and mechanical properties were achieved.

Table 3.1. *Sintering parameters employed in this study in air at 1 atm.*

TOTAL TIME (MIN)	TIME TO TEMP (MIN)	TEMP (°C)	PHASE
0	0	25	Ramp 1
240	240	240	Ramp 1
720	60	300	Burnout
1173	333	1271	Ramp 2
1178	5	1271	Sintering hold
1238	60	900	Cool down
1688	450	25	Cool down

Subsequently, the Cool Down phase was employed to relieve thermal stresses and stabilize the sintered material. The temperature was gradually reduced from 1271°C to 900°C over 60 minutes, followed by a further decrease to ambient temperature over 450 minutes, making a total of 1688 minutes for the complete process to occur. This controlled cooling rate helped prevent thermal shock and internal stresses, preserving the structural integrity and performance of the final product. Through meticulous control of each stage of the sintering process, the research aimed to optimize the microstructure and properties of the material,

laying the foundation for achieving desired performance characteristics for various applications.

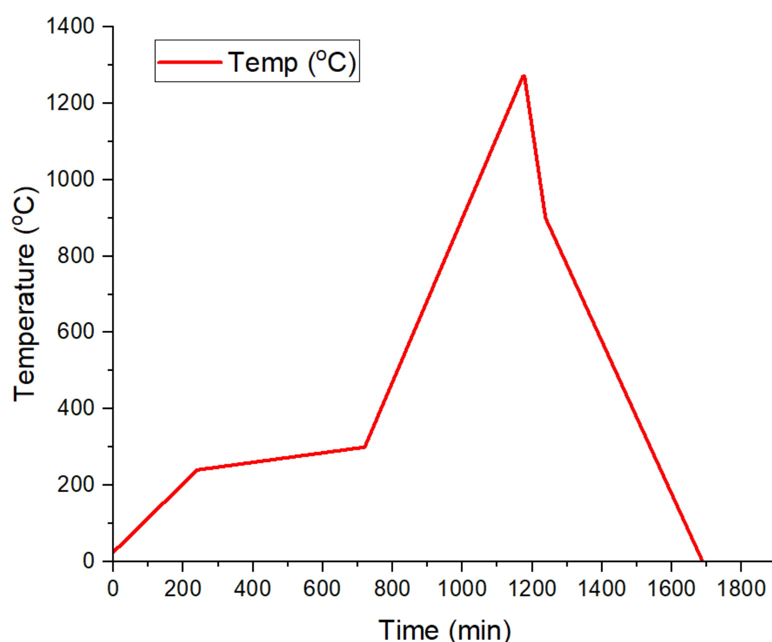

Figure 3.3. *Graph showing the temperature variation profile during sintering process.*

3.4. Printing of Silver Conductive Designs

3.4.1. Preparation of Silver Paste

To prevent contaminating the nano-silver paste and decreasing its effectiveness, it was prepared in a generally clean area, to avoid the introduction of contaminants. Silver paste contains 2 components - silver powder and an organic vehicle.

3.4.2. Deposition of Silver Paste

The Voltera V-One printing system was utilized to deposit silver conductive designs onto the ceramic substrates. Specialized silver conductive paste was employed for this purpose, chosen for its high conductivity and compatibility with the printing system. The printing process enabled the creation of precise conductive pathways tailored to the specific

requirements of electronic circuitry. Three sample silver ceramic connectors were fabricated with single, double, and triple prints named as SCC-1 (single print), SCC-2 (double print), and SCC-3 (triple print) to determine the impact of printing density (thickness of silver paste) on the properties of connectors.

3.5. Characterization of Silver Conductive Connectors

By employing a comprehensive suite of characterization techniques, including conductivity testing, adhesion testing, and microscopy analysis, a thorough assessment of the printed silver conductive connectors was achieved. These characterization efforts were instrumental in elucidating the suitability of the connectors for high-temperature electronic applications, contributing to the advancement of ceramic-based passive components and system integration in high-power electronics modules.

3.5.1. Conductivity Testing

Conductivity testing was conducted to evaluate the electrical performance of the printed silver conductive connectors. In the conductivity testing, the digital multimeter was connected to the terminals of the printed silver conductive connectors, ensuring proper calibration for accurate resistance measurements. A low-level voltage was applied across the terminals, and voltage and corresponding current readings were recorded from the multimeter. Using Ohm's law, the resistance of the conductive pathway was calculated. Multiple measurements were taken at different points along the conductive pathway to assess uniformity and consistency. The resistance values were recorded and analyzed to assess the suitability of the silver conductive paste for high-temperature applications.

3.5.2. Adhesion Testing

The ASTM-D3359 standard was used to carry out the adhesion peel test. Samples were cured

at 200 degree Celsius for 30 minutes before starting on the adhesion test. Following the creation of the 6-cut, pressure-sensitive tape, specifically Permacel P-99 tape with a peel strength of 6.67 N/cm (61 oz/in), was applied uniformly over the cut. The tape was carefully pressed onto the surface to ensure proper adhesion. A universal testing machine, calibrated to apply a controlled force, was utilized to measure the peel force required to remove the tape from the sample surface. Peel force was recorded and the sample thickness was measured with digital caliper.

CHAPTER 4 RESULTS AND DISCUSSION

4. Introduction

In this chapter, the experimentation and analysis are presented. The focus of this investigation lies in the fabrication and evaluation of high-temperature ceramic silver connectors designed for advanced electronic applications. Through AM manufacturing processes and characterization techniques, connectors designed for durability, conductivity, and thermal resilience are investigated. These endeavors encompassed the precise fabrication of ceramic substrates, the deposition of silver conductive designs, and the evaluation of key properties, such as electrical conductivity, adhesion strength, and microstructural integrity. The results presented herein provide an assessment of the performance and suitability of the fabricated connectors for high-temperature electronic environments.

4.1.Printing of Conductive Silver Paste on Ceramics

This research was centered around the development of a nano silver paste-ceramic connector, leveraging advanced manufacturing techniques. The primary objective lies in combining the benefits of ceramic material, 3D printing technology, and silver coating to create a connector that excels in charge carrying capacity, temperature resilience, and overall reliability.

In the initial phase of the study, ceramic material was fabricated using 3D printing technology. The next crucial step involved the application of silver coating onto the ceramic surface using the Voltera V-One printer. Silver paste is chosen for its superior conductivity, making it an ideal material for electrical connections. The direct deposition of silver paste onto the ceramic eliminates the need for traditional assembly methods, thereby streamlining the manufacturing process and enhancing the efficiency of the connector production. Moreover, the silver paste coating serves a dual purpose by not only improving the electrical conductivity of the connector but also refining the surface roughness of the ceramic with

potential applications spanning across industries like electronics, aerospace, defense, energy, and automotive sectors. To ensure the practical viability of the connector, the research aimed to determine the temperature range at which it can be effectively deployed in real-world applications. This involves testing and evaluation procedures to assess the connector's performance under varying temperature conditions, thereby validating its reliability and stability across a range of operational environments. SCC-1 (single print of silver paste) was produced using a flow of X and a sintering temperature of 200 C, SCC-2 (double print of silver paste) was produced using a flow of Y and a sintering temperature of A, and SCC-3 (triple print of silver paste) was produce using a flow of X and a sintering temperature of B.

Figure 4.1 shows the successful printing of silver paste on the surface of the ceramic in three samples called SCC-1, SCC-2, and SCC-3. The images show a dense layer of silver conductive paste (the darker region) bonded to a lighter, ceramic substrate. The layers comprise parallel silver paste lines (patterns) deposited on the ceramic substrate. These silver paste lines exhibit uniform thickness and spacing, demonstrating precise manufacturing, although slight irregularities are also visible (as indicated by arrows), arising from the deposition process. These imperfections could be related to likelihood that flow of the silver paste gets disturbed causing small gaps or substrate surface irregularities or contamination might have hindered proper adhesion of the silver paste, leading to disturbed patterning. The quality of the silver paste layer affects electrical performance. Smoother surfaces minimize resistance. The connector’s design was ensured for reliable electrical contact and efficient heat dissipation.

The scale of the microscopic images for all the three samples shows the thickness of the silver paste at various points along the cross-section on the surface of the ceramic substrate. The average thickness values range from 90 µm to 200 µm due to successive addition of the silver paste printed on the surface of ceramic. The values shown suggest that the silver layer

is uniformly distributed throughout its thickness. The length of a separated single layer of silver paste has shown to be around 1000 µm. Each silver paste line's thickness, spacing, and length is critical for performance.

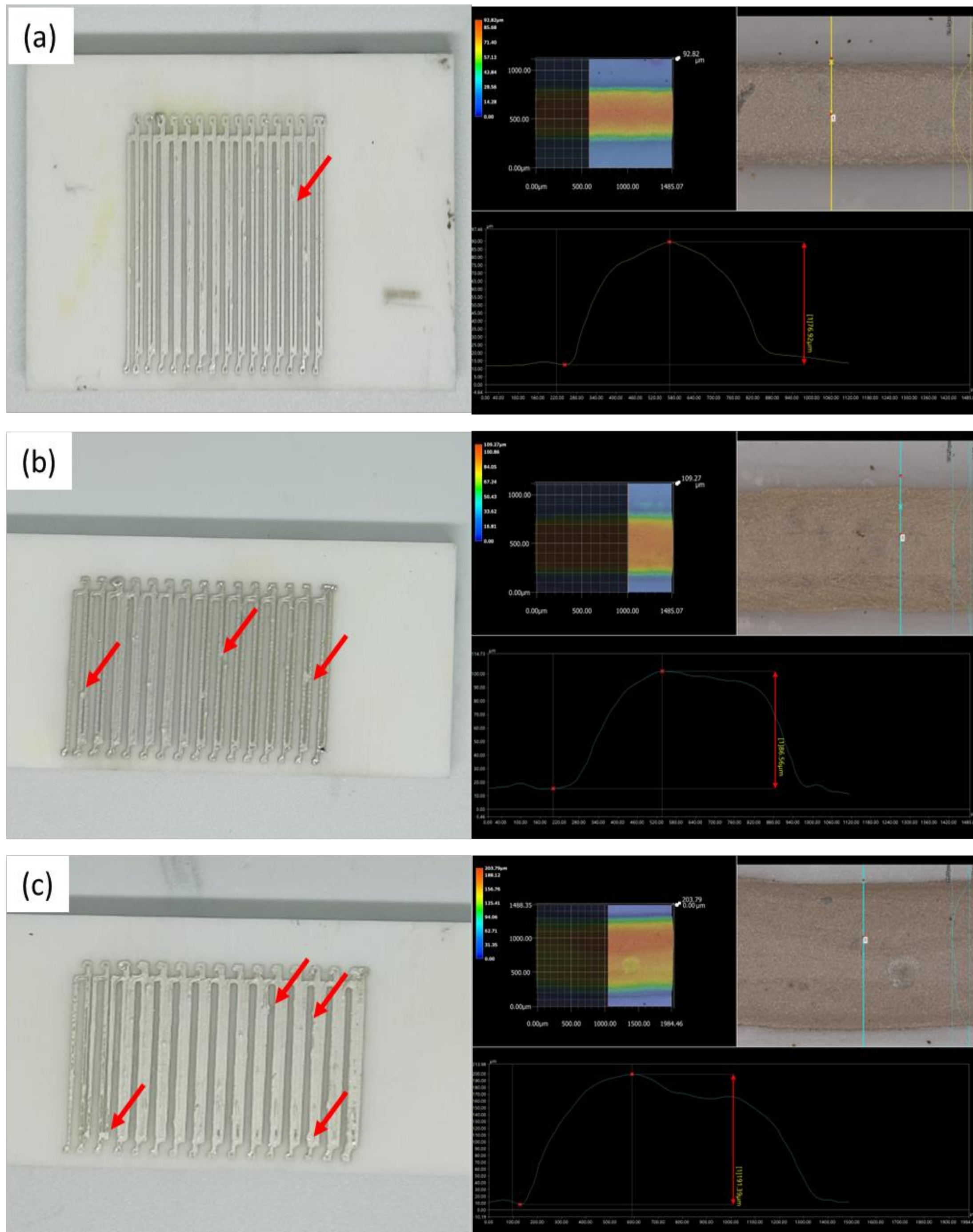

Figure 4.1. *Images (left) showing the printed silver paste conductive design on ceramic (a) SCC-1, (b) SCC-2, and (c) SCC-3 and microscopic images (right) of sections of printed silver paste.*

4.2.Conductivity of the Printed Silver paste

The electrical conductivity of the silver paste layer is critical, as it governs the overall performance of the high-temperature ceramic silver paste connectors [109]. Conductivity is inversely related to resistivity, which depends on factors like the silver paste layer's microstructure, defects, and impurities. Minimizing resistance is crucial for reducing power losses. This can be achieved by optimizing the conductivity (or minimizing the resistivity) of the well-sintered, dense silver paste layer through careful control of the sintering process and minimizing defects and impurities. The data points in the graph shown in Figure 4.2(a) show that the resistance of the conductor increases as the distance increases. This is to be expected, as longer conductors have more material for the current to flow through, which makes it more difficult for the current to flow. The trendline appears to be approximately linear which is a desirable property and suggests a uniform distribution of the silver paste onto the ceramic substrate. Overall, the graph demonstrates that there is a positive correlation between resistance and distance in the printed silver paste conductor. This means that as the distance increases, the resistance also increases.

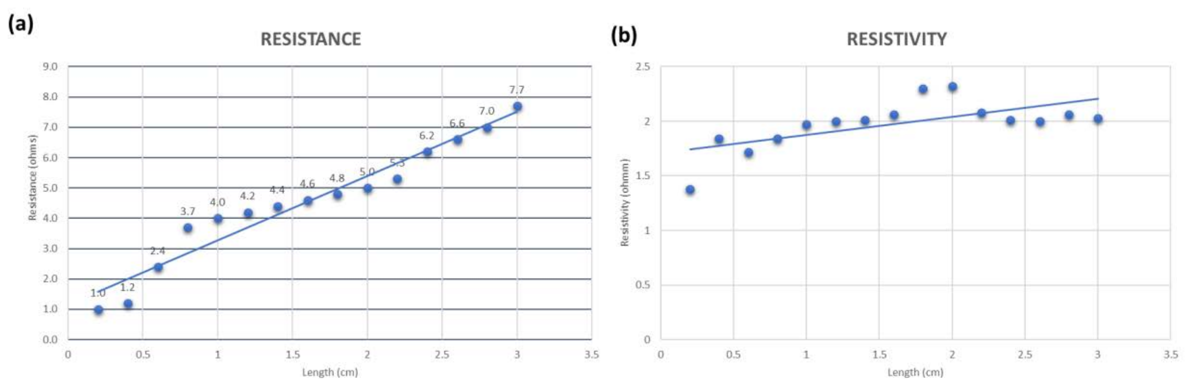

Figure 4.2 *Relationship between **(a)** Resistance vs Length, **(b)** Resistivity vs Length of SCC-1.*

Similarly, the resistivity of the conductor increases as its length increases (Figure 4.2b). This

is because longer conductors have more material for the current to flow through, which increases the resistance [110]. The slight variability in the data points variability could be due to factors such as variations in the thickness or width of the conductor, or imperfections in the material at the nanoscale.

Overall, the graph confirms what is expected from the basic principles of electrical conductivity: the resistance of a conductor is directly proportional to its length. The specific values of the resistivity and the slope of the line will depend on the material properties of the conductor, such as the bulk resistivity of silver and the cross-sectional area of the conductor. However, Figure 4.2a concentrates on the specific resistance exhibited by a particular conductor sample at varying distances, while Figure 4.2b shows the variations of resistivity with length. As resistivity is the intrinsic property of each material and should show constant trend throughout the length of the connector [111]. However, instead of a constant behavior a slight variations have been observed in the resistivity of the silver paste along the length by showing a slight increase initially with a subsequent relatively constant trend. This behavior could be attributed to factors such as the alignment and arrangement of the conducting lines, as well as any potential structural changes at various points along the length of the conducting design.

Table 4.1 and Figure 4.3 shows the conductivity performance of SCC-1, SCC-2, and SCC-3. Upon examination of the resistance values at various distances for each sample, a consistent trend emerges: as the distance increases, so does the resistance, reflecting the typical behavior of electrical circuits. However, the comparison of resistance values at equivalent distances among the samples reveals significant insights. Notably, SCC-3 consistently exhibits the lowest resistance, followed by SCC-2 and then SCC-1, indicating that increasing the thickness of the silver coating via multiple printings effectively reduces resistance and enhances conductivity. This finding underscores the principle that thicker coatings provide more pathways for electron flow, thereby diminishing resistance.

Table 4.1. *Resistance vs distance values for all the three samples i.e. SCC-1 to SCC-3.*

	SCC-1		SCC-2		SCC-3	
POINT	Resistance (ohms)	DISTANCE (cm)	Resistance (ohms)	DISTANCE (cm)	Resistance (ohms)	DISTANCE (cm)
Initial line	1.0	0.2	0.6	0.2	0.3	0.2
initial & 2nd line	1.2	0.4	1.0	0.4	0.3	0.4
initial & 3rd line	2.4	0.6	1.6	0.6	0.5	0.6
initial & 4th line	3.7	0.8	2.0	0.8	0.3	0.8
initial &5th line	4.0	1.0	2.2	1.0	0.3	1.0
initial & 7th line	4.2	1.2	2.4	1.2	0.3	1.2
initial & 8th line	4.4	1.4	2.8	1.4	0.3	1.4
initial & 9th line	4.6	1.6	3.2	1.6	0.4	1.6
initial & 10th line	4.8	1.8	3.4	1.8	0.4	1.8
initial & 11th line	5.0	2.0	3.6	2.0	0.4	2.0
initial&12th line	5.3	2.2	4.0	2.2	0.6	2.2
initial &13th line	6.2	2.4	4.5	2.4	0.4	2.4
initial & 14th line	6.6	2.6	5.0	2.6	0.6	2.6
initial & 15th line	7.0	2.8	5.3	2.8	1.0	2.8
initial & 16th line	7.7	3.0	5.5	3.0	1.6	3.0

However, in the SCC-3, there comes a point where resistance tends to increase after a certain distance. Moreover, the diminishing returns observed from SCC-2 to SCC-3 suggest a saturation point in conductivity or limitations inherent in the printing process. Thus, while increasing thickness improves performance, there are practical considerations such as material cost, production time, and optimization trade-offs that must be carefully balanced. Figure 4.3b shows the behavior of resistivity vs length of all three samples. As resistivity is the intrinsic property of the material ad theoretically should show constant value at various points. However, the graphs for all three samples show fluctuations in resistivity at various points hinting at the defects in the 3D printing of the silver paste. However, the overall resistivity trend shows a higher value for SCC-1 as compared to SCC-2 and SCC-3 showing least conductive performance of the SCC-1 as compared to other samples.

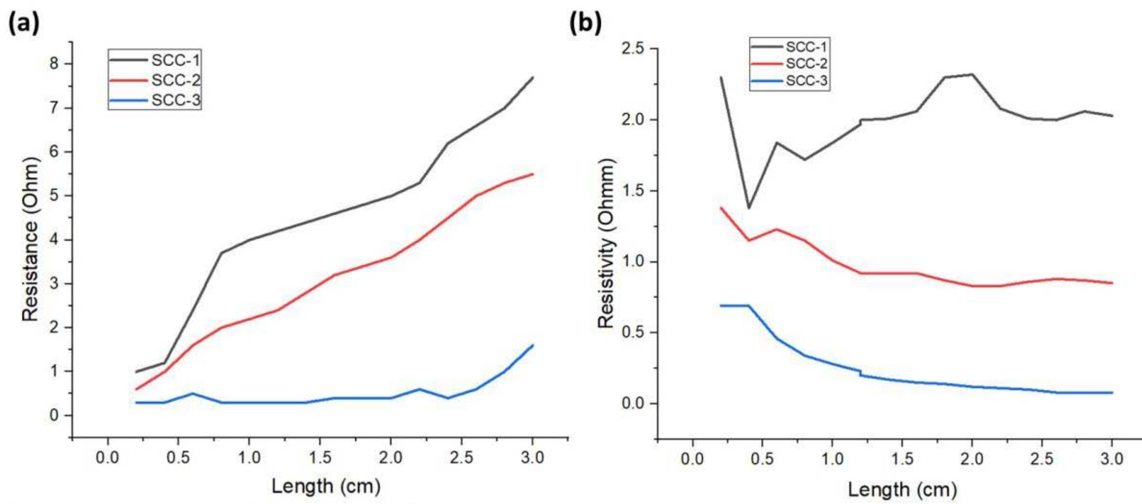

Figure 4.3 *Graph showing the* ***(a)*** *resistance vs length and* ***(b)*** *resistivity vs length trend for SCC-1 to SCC-3.*

Table 4.2 and Figure 4.4 represent the resistance measurements of SCC-1 after curing the connector at three different temperatures: 200°C, 300°C, and 400°C. This approach aims to understand how the curing temperature influences the electrical properties of the connector.

The resistance values of SCC-1 range from 1.9 - 27.7 Ohms over distances from 0.2 - 3.2 cm after curing at 200°C. The resistance values range from 1.2 - 23 Ohms over similar distances after curing at 300°C. The resistance values range from 2 - 2.9 Ohms over the same distances after curing at 400°C. When comparing the curing temperatures, 200°C produces the highest resistance as compared to the other curing temperatures, while 400°C produces the lowest resistance.

Lower resistance values after curing at 400°C indicate improved conductivity compared to curing at lower temperatures. This suggests that higher curing temperatures enhances the bonding and conductivity of the silver paste, resulting in lower resistance. The data demonstrates that curing at 200°C may not be optimal for achieving the desired electrical

performance. Based on the resistance measurements, curing at 400°C appears to be more effective in achieving lower resistance values, indicating better conductivity.

Table 4.2. *Resistance vs distance values for SCC-1 cured at three different temperatures.*

At 200 °C		At 300 °C		At 400 °C	
Distance (cm)	Resistance (Ohm)	Distance (cm)	Resistance (Ohm)	Distance (cm)	Resistance (Ohm)
0.2	1.9	0.2	1.2	0.2	2
0.4	2.9	0.4	1.8	0.4	2.4
0.6	5	0.6	3.6	0.6	2.7
0.8	7.5	0.8	5	0.8	2.8
1	9.4	1	6.9	1	3.3
1.2	10.6	1.2	8.6	1.2	2.7
1.4	12.6	1.4	10.2	1.4	2.5
1.6	14.7	1.6	11.2	1.6	2.4
1.8	16.7	1.8	13	1.8	2.3
2	18.5	2	14.5	2	2.7
2.2	19.1	2.2	15.4	2.2	2.5
2.4	21.5	2.4	16.9	2.4	2.8
2.6	22.3	2.6	19.1	2.6	2.9
2.8	24.2	2.8	20	2.8	2.9
3	25.2	3	21.8	3	2.9
3.2	27.7	3.2	23	3.2	2.7

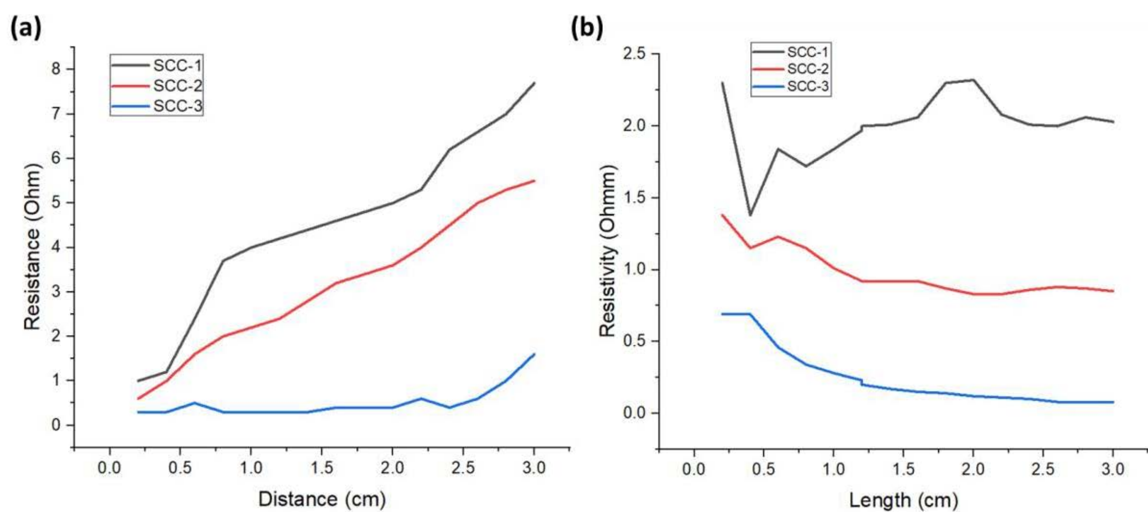

Figure 4.4. *Graph showing the trend lines for resistance vs distance for SCC-1 cured at three different temperatures.*

4.3. Adhesion Testing of Conductive silver paste on Ceramic

Adhesion testing is a critical step in evaluating the performance of these connectors, as the connectors need to form strong and durable bonds with the ceramic substrate to ensure reliable electrical performance. There are several different methods for adhesion testing, but a common method is the peel adhesion test. In a peel adhesion test, a force is applied to the interface between the connector and the substrate in a direction that is parallel to the surface of the substrate after placing an adhesion tape on it. The force required to debond the peel tape from the substrate is measured and used to assess the adhesion strength. The specific setup for an adhesion test will vary depending on the testing method and the materials being tested. Figure 4.5 shows the adhesion testing setup employed in this study. The machine can apply a load of “100N” and has clamps/fixtures present to securely hold the test samples in place. The load was adjusted with the knob to attempt peel off the tape from the silver connector surface.

Figure 4.5. *Setup of Adhesion Apparatus.*

The data from an adhesion test can be used to assess the strength and durability of the printed silver layer on the surface of substrate. This information is essential for ensuring the reliability of high temperature ceramic silver connectors in various applications.

4.4.Adhesion Results Analysis

A peel adhesion test of a printed silver conductor on a ceramic substrate is shown in Figure 4.6 (a, b) for SCC-1 and SCC-2, respectively. The silver pattern was sliced in a lattice pattern with six cuts (as shown with yellow arrow) in each direction. The lattice was then covered with pressure-sensitive tape (as shown with red arrow).

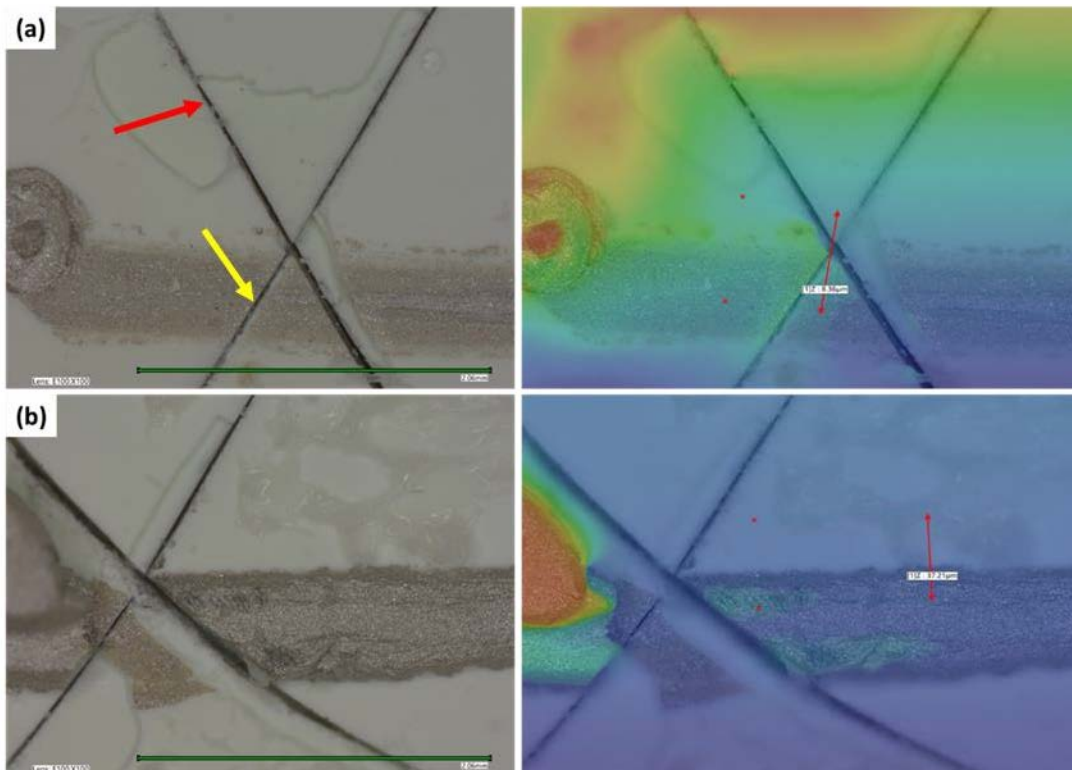

Figure 4.6. *Adhesion analysis of SCC-1 and SCC-2*

The graphs in Figure 4.7 depict the results of peel adhesion tests conducted on printed silver conductors bonded to ceramic substrates, for SCC-1 and SCC-2, respectively. The x-axis represents the extension (mm), while the y-axis represents the applied load (N). As can be seen, by increasing the load, extension is being produced until reaching a maximum limit where there is no further increase in the load applied due to maximum extension produced in the applied tape without peeling.. In other words, the maximum load achieved is the point where there is resistance started in peeling off of the applied layer. By comparing the graph of SCC-

1 (Fig. 4.7a) with SCC-2 (Fig. 4.7b), it is found that the maximum force applied by retaining the adhesion is higher (3.45 N) in case of SCC-2 than the maximum force applied in case of SCC-1 (1.4 N) which means it was more securely bonded in case of SCC-2.

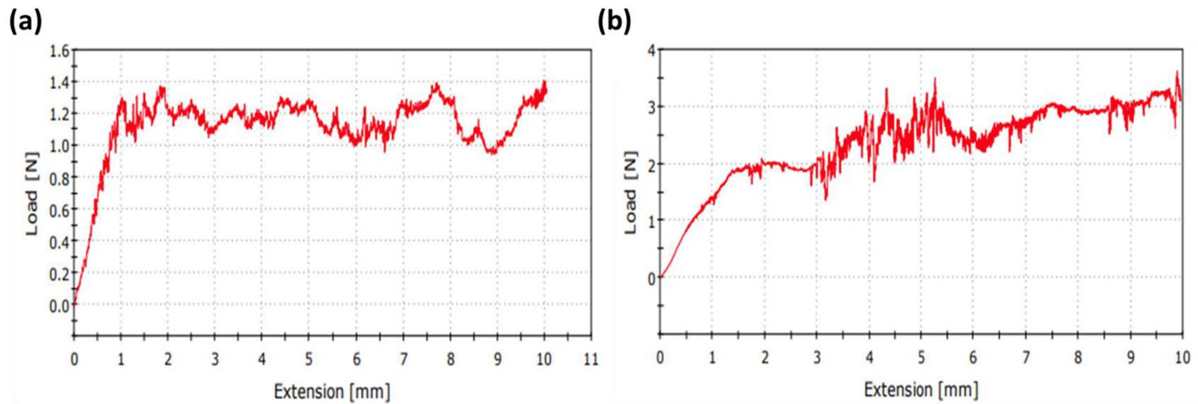

Figure 4.7: *Results of Adhesion Test for (a) SCC-1 and (b) SCC-2.*

This implies that the debonding in case of SCC-2 is more difficult to achieve as compared to SCC-1. The fluctuations in the graph lines show the partial debonding occurred at various points along the silver paste lines. These shows the tape was extended by applying the force at various points along the silver lines without getting debonded from the surface of the ceramic. Such behavior could result from slight variations in the adhesion strength of layer along the cross-section. Similar pattern of peel adhesion tests have been obtained in previous studies [112, 113]. Overall, both samples exhibit adhesion between the printed silver conductor and the ceramic substrate, but SCC-2 demonstrates a stronger and more consistent adhesive bond compared to SCC-1. This suggests that by printing multiple layers of silver paste onto the ceramic substrate in silver ceramic connectors, the mechanical properties would be enhanced.

5. Discussion

The present research work focused on the fabrication and comprehensive performance

analysis of high-temperature ceramic silver paste connectors, which are critical components in various industries requiring reliable electrical connections under extreme temperature conditions. Through a systematic experimental approach, the fabrication process was studied, and the connectors' performance characteristics were evaluated.

The research was conducted to develop a novel approach for applying a uniform, smooth layer of silver paste to ceramic substrates, particularly focusing on surface roughness and deposition density. In this pursuit, we explored the efficacy of utilizing silver paste deposition, a method intended to mitigate the challenges associated with rough surfaces commonly encountered in traditional connector fabrication methods. Thus, the thesis lays the groundwork for investigating the fabrication and evaluation of high-temperature ceramic silver paste connectors.

Conductivity testing, adhesion testing, and microscopy showed successful deposition and functionality of the silver connectors with high precision and desirable properties. Particularly adhesion testing showed the silver paste has been deposited and well adhered to the surface of the ceramic [114]. The conductivity tests performed on the fabricated connectors demonstrated their excellent electrical properties, exhibiting low resistance and high conductivity consistent with previous reports of silver paste deposition for electrode performance [114, 115]. The resistance and resistivity measurements further validated these findings, confirming the suitability of these connectors for high-temperature applications. The conductivity tests further showed that SCC-3 (triple printed) silver ceramic connector has the lowest resistance to the flow of current as compared to SCC2 and SCC-1, which means its electrical properties are superior to other connectors. This could be owing to the increased cross-sectional area available for the flow of current through SCC-3 as compared to SCC-2 and SCC-1. While thicker coatings may offer better performance, they also require more resources and time during the manufacturing process. Furthermore, it was shown that

the connector which was cured at higher temperature (400 ^{o}C) showed better electrical conductance as compared to curing as lower temperatures. This is important as these connectors are used in a variety of applications that require high temperature stability, such as in the automotive and aerospace industries [116]. The specific properties of high temperature ceramic silver paste connectors [117] will vary depending on the materials used and the manufacturing process [118].

The peel adhesion tests revealed strong bonding between the ceramic and silver components particularly in the case of SCC-2, with a double print as compared to single print ensuring mechanical integrity and durability under operating conditions. Thicker layers may show better adhesion because they provide more contact points and a larger surface area for bonding and or first layer could have activated the surface after first printing for better adhesion. The results of adhesion testing particularly show the importance of achieving strong and consistent adhesive bonds in high-temperature ceramic silver connectors. The observed variations in adhesion strength between samples SCC-1 and SCC-2 highlight the influence of printing parameters on the adhesive bond. These findings underscore the need for meticulous control and optimization of fabrication processes to ensure reliable and robust connector performance in real-world applications. The combination of robust electrical and mechanical properties makes these ceramic silver connectors a promising solution for demanding high-temperature applications in industries such as aerospace, automotive, and power generation.

CHAPTER 5 CONCLUSIONS AND RECOMMENDATIONS

In conclusion, the investigation into high-temperature ceramic silver connectors has illuminated promising avenues for enhancing electronic connectivity in demanding environments. Through fabrication processes and evaluation, this study has shed light on the efficacy of additive manufacturing techniques in overcoming traditional manufacturing constraints.

A series of carefully orchestrated steps designed to ensure the quality, reliability, and functionality of the fabricated connectors were performed. The choice of amorphous fused silica ceramic photopolymer resin from Formlabs, Inc. represents a deliberate consideration for high-temperature resilience and compatibility with AM techniques. This resin, infused with silica-filled ceramic particles, serves as the foundational material for the fabrication of ceramic substrates. The photopolymer resin was precisely deposited layer by layer, facilitated by a Formlabs 3D printing machine. This process enabled the creation of intricate ceramic structures with precise dimensions and geometries, which are essential for optimizing thermal and electrical conductivity in the final connectors.

The deposition of silver conductive designs onto the ceramic substrates represents a pivotal phase. Utilizing the Voltera V-One printing system and specialized silver conductive paste, precise conductive pathways were created on the substrates. The deposition process was controlled to ensure uniformity and precision in the placement of the conductive designs, thereby optimizing electrical conductivity and performance of the connectors. Three variations of the silver connectors were fabricated by printing single, double, and triple layers of silver paste to understand its impact on the properties of the silver connectors.

The amalgamation of ceramic substrates and silver conductive designs represents a novel approach to addressing the challenges posed by high temperatures and mechanical stress. By

leveraging the precision of 3D printing and the conductivity of silver, this research has demonstrated the feasibility of creating robust silver connectors. The results obtained from conductivity testing and adhesion analysis underscore the importance of material selection and processing parameters in achieving optimal performance.

The findings of this research contribute to the field of high-temperature connector technology, providing valuable insights into the fabrication methods and performance characteristics of ceramic silver connectors. The optimized fabrication process and the comprehensive performance analysis lay a solid foundation for further advancements and widespread adoption of these connectors in various industries.

While the results obtained in this study are promising, there is still room for further research and improvement. Future studies could explore alternative materials or material combinations, thereby investigating potential cost-effective manufacturing techniques for large-scale production.

5.1. Recommendations

Based on the findings and insights gathered from the research conducted on the fabrication and evaluation of high-temperature ceramic silver paste connectors for advanced electronic applications, several recommendations are proposed:

Further research is recommended to explore and optimize the sintering parameters, including temperature profiles, ramp rates, and hold times, to achieve enhanced material properties such as electrical conductivity, mechanical strength, and thermal stability. For instance, flow rate should be controlled to deposit a uniform layer of the silver paste which would cause a consistent mechanical properties of the connector throughout the silver paste length. Moreover, it is recommended to change the ramp rate including the time for curing silver paste which has been shown to enhance the electrical conductive performance of connectors.

A much higher temperature than 400 ^{o}C could degrade the silver paste so it is recommended to increase the time for curing of silver paste. Surface treatments, adhesion promoters, and interfacial bonding techniques should be explored to improve reliability and longevity. Therefore, expand the investigation by increasing the number of samples to encompass a wider range of sintering parameters. By systematically varying parameters such as temperature profiles, ramp rates, and hold times, a more comprehensive understanding of their impact on the material properties can be attained.

Further, it is desirable to employ advanced microscopy techniques such as transmission electron microscopy (TEM) and atomic force microscopy (AFM) to perform in-depth analysis of the microstructure of the ceramic silver connectors. This will enable the precise characterization of grain boundaries, crystallographic orientation, and defect structures, shedding light on the underlying mechanisms governing the material properties and performance.

Moreover, it is also important to explore opportunities for integrating high-temperature ceramic silver paste connectors into advanced electronic systems, such as power electronics, aerospace applications, and automotive electronics. Collaboration with industry partners and research institutions to identify specific application requirements and develop tailored solutions would be beneficial. It would be beneficia to conduct comprehensive studies to assess the complete functionality of the ceramic silver paste connectors in real-world electronic applications. Evaluating their performance under simulated operating conditions is imperative. This will provide valuable feedback on factors such as thermal cycling, mechanical stress, and long-term reliability, guiding further improvements and optimizations.

References

[1] J.S. Reed, Principles of ceramics processing, (1995).
[2] R. Pampuch, A Brief History of Ceramic Innovation, in: R. Pampuch (Ed.), An Introduction to Ceramics, Springer International Publishing, Cham, 2014, pp. 1-17.
[3] W.A. Oldfather, A note on the Etymology of the word "ceramic" 1, 2, Journal of the American Ceramic Society 3(7) (1920) 537-542.
[4] F. Ernst, O. Kienzle, M. Rühle, Structure and composition of grain boundaries in ceramics, Journal of the European Ceramic Society 19(6-7) (1999) 665-673.
[5] S. Kume, M. Yasuoka, S.-K. Lee, A. Kan, H. Ogawa, K. Watari, Dielectric and thermal properties of AlN ceramics, Journal of the European Ceramic Society 27(8-9) (2007) 2967-2971.
[6] J. Rödel, A.B.N. Kounga, M. Weissenberger-Eibl, D. Koch, A. Bierwisch, W. Rossner, M.J. Hoffmann, R. Danzer, G. Schneider, Development of a roadmap for advanced ceramics: 2010–2025, Journal of the European Ceramic Society 29(9) (2009) 1549-1560.
[7] V.A. Greenhut, Properties of Ceramics and Glasses, (1997).
[8] H. Hennicke, A. Hesse, Traditional Ceramics, Concise Encyclopedia of Advanced Ceramic Materials, Elsevier1991, pp. 488-494.
[9] R. Haubner, M. Herrmann, B. Lux, G. Petzow, R. Weissenbacher, M. Wilhelm, High performance non-oxide ceramics II, Springer2003.
[10] L. Black, P. Purnell, J. Hill, Current themes in cement research, Advances in Applied Ceramics 109(5) (2010) 253-259.
[11] A.O. Shepard, Ceramics for the Archaeologist, Carnegie Institution of Washington Washington, DC1956.
[12] R. van Nieuwenhoven, M. Drack, I. Gebeshuber, Engineered Materials: Bioinspired "Good Enough" versus Maximized Performance, Advanced Functional Materials (2023).
[13] S. Somiya, Handbook of advanced ceramics: materials, applications, processing, and properties, Academic press2013.
[14] P.F. Manicone, P.R. Iommetti, L. Raffaelli, An overview of zirconia ceramics: basic properties and clinical applications, Journal of dentistry 35(11) (2007) 819-826.
[15] R.G. Breckenridge, W.R. Hosler, Electrical properties of titanium dioxide semiconductors, Physical Review 91(4) (1953) 793.
[16] M. Bengisu, M. Bengisu, Engineering ceramics, Springer2001.
[17] FactMR, CeramicMarket Outlook, (2024-2034), (2024).
[18] F.B. Insights, [Latest Report] The global advanced ceramics market report size is projected to reach USD 1,80,463.4 million by 2028 at a CAGR of 10.2%.... Read More at:- https://www.fortunebusinessinsights.com/advanced-ceramics-market-105073, (2021).
[19] Superbloov, (2023).
[20] H. Takemura, H. Fukushima, Recent trends of advanced ceramics industry and Fine Ceramics Roadmap 2050, International Journal of Applied Ceramic Technology 20(2) (2023) 681-688.
[21] D. Kujanen, Technical ceramics and refractories applications and volumes literature review, (2019).
[22] M.U. Iqbal, A. Hussain, M. Shahid, M. Ramzan, A. Karim, M. Akhtar, Processing of Bioceramics by Pressing and Tape Casting, Advanced Bioceramics, CRC Press, pp. 74-93.
[23] M. Dadkhah, J.-M. Tulliani, A. Saboori, L. Iuliano, Additive manufacturing of ceramics: Advances, challenges, and outlook, Journal of the European Ceramic Society (2023).
[24] I. Gibson, D.W. Rosen, B. Stucker, M. Khorasani, D. Rosen, B. Stucker, M. Khorasani, Additive manufacturing technologies, Springer2021.
[25] E. Fiume, B. Coppola, L. Montanaro, P. Palmero, Vat-photopolymerization of ceramic materials: exploring current applications in advanced multidisciplinary fields, Frontiers in Materials 10 (2023).
[26] Z. Chen, Z. Li, J. Li, C. Liu, C. Lao, Y. Fu, C. Liu, Y. Li, P. Wang, Y. He, 3D printing of ceramics: A review, Journal of the European Ceramic Society 39(4) (2019) 661-687.
[27] R.W. Johnson, J.L. Evans, P. Jacobsen, J.R. Thompson, M. Christopher, The changing automotive environment: high-temperature electronics, IEEE transactions on electronics packaging manufacturing 27(3) (2004) 164-176.
[28] J. Watson, G. Castro, High-temperature electronics pose design and reliability challenges,

Analog Dialogue 46(2) (2012) 3-9.
[29] H. Jdidi, N. Fourati, C. Zerrouki, L. Ibos, M. Fois, A. Guinault, W. Jilani, S. Guermazi, H. Guermazi, Exploring the optical and dielectric properties of bifunctional and trifunctional epoxy polymers, Polymer 228 (2021) 123882.
[30] K. Pielichowska, K. Pielichowski, Thermal Analysis in Energy, Thermal Analysis of Polymeric Materials: Methods and Developments 2 (2022) 533-559.
[31] J.-Y. Pei, S.-L. Zhong, Y. Zhao, L.-J. Yin, Q.-K. Feng, L. Huang, D.-F. Liu, Y.-X. Zhang, Z.-M. Dang, All-organic dielectric polymer films exhibiting superior electric breakdown strength and discharged energy density by adjusting the electrode–dielectric interface with an organic nano-interlayer, Energy & Environmental Science 14(10) (2021) 5513-5522.
[32] D. Wang, Solenoid Power Inductor with Ferrite/Insulator Films based on Kapton, Northeastern University, 2020.
[33] R. Riedel, W. Dressler, Chemical formation of ceramics, Ceramics International 22(3) (1996) 233-239.
[34] S.R. Kandavalli, S.R. Kandavalli, R.S. Ruban, C.H. Lo, R. Kumar, C.I. Pruncu, a conceptual analysis on ceramic materials used for dental practices: manufacturing techniques and microstructure, ECS Journal of Solid State Science and Technology 11(5) (2022) 053005.
[35] Y. Zhao, G. Shi, J.-T. Miao, R. Liu, X. Sang, Preparation of hierarchically porous calcium hexaaluminate ceramics through in-situ gelation-assisted direct ink writing, Ceramics International (2024).
[36] V. Babashov, N. Varrik, Gel Casting Method for Producing Ceramic Materials: A Review, Glass and Ceramics 80(1) (2023) 9-16.
[37] A. Ruys, J. Kerdic, C. Sorrell, Thixotropic casting of ceramic-metal functionally gradient materials, Journal of materials science 31 (1996) 4347-4355.
[38] S. Shahrestani, M.C. Ismail, S. Kakooei, M. Beheshti, Effect of additives on slip casting rheology, microstructure and mechanical properties of Si3N4/SiC composites, Ceramics International 46(5) (2020) 6182-6190.
[39] L. Santos, J. Silva, J. Cartaxo, A. Rodrigues, G. Neves, R. Menezes, Freeze-casting applied to ceramic materials: a short review of the influence of processing parameters, Cerâmica 67 (2021) 1-13.
[40] L. Yu, M. Kanezashi, H. Nagasawa, T. Tsuru, Phase inversion/sintering-induced porous ceramic microsheet membranes for high-quality separation of oily wastewater, Journal of Membrane Science 595 (2020) 117477.
[41] M. Vajdi, F.S. Moghanlou, F. Sharifianjazi, M.S. Asl, M. Shokouhimehr, A review on the Comsol Multiphysics studies of heat transfer in advanced ceramics, Journal of Composites and Compounds 2(2) (2020) 35-43.
[42] C.L. Cramer, E. Ionescu, M. Graczyk-Zajac, A.T. Nelson, Y. Katoh, J.J. Haslam, L. Wondraczek, T.G. Aguirre, S. LeBlanc, H. Wang, Additive manufacturing of ceramic materials for energy applications: Road map and opportunities, Journal of the European Ceramic Society 42(7) (2022) 3049-3088.
[43] T. Moritz, S. Maleksaeedi, Additive manufacturing of ceramic components, Additive manufacturing, Elsevier2018, pp. 105-161.
[44] J.S. Pelz, N. Ku, M.A. Meyers, L.R. Vargas-Gonzalez, Additive manufacturing of structural ceramics: a historical perspective, Journal of Materials Research and Technology 15 (2021) 670-695.
[45] A. Martínez-García, M. Monzón, R. Paz, Standards for additive manufacturing technologies: Structure and impact, Additive manufacturing, Elsevier2021, pp. 395-408.
[46] J.S. Pelza, N. Ku, M.A. Meyers, L. Vargas-Gonzalez, Additive manufacturing of structural ceramics: a historical perspective, Journal of materials research and technology 15 (2021) 670-695.
[47] Y. Lakhdar, C. Tuck, J. Binner, A. Terry, R. Goodridge, Additive manufacturing of advanced ceramic materials, Progress in Materials Science 116 (2021) 100736.
[48] I. Gibson, D.W. Rosen, B. Stucker, I. Gibson, D.W. Rosen, B. Stucker, Sheet lamination processes, Additive manufacturing technologies: rapid prototyping to direct digital manufacturing (2010) 223-252.
[49] J.K. Placone, A.J. Engler, Recent advances in extrusion-based 3D printing for biomedical applications, Advanced healthcare materials 7(8) (2018) 1701161.
[50] I. Gibson, D. Rosen, B. Stucker, M. Khorasani, I. Gibson, D. Rosen, B. Stucker, M. Khorasani,

Binder jetting, Additive manufacturing technologies (2021) 237-252.
[51] F. Zhang, L. Zhu, Z. Li, S. Wang, J. Shi, W. Tang, N. Li, J. Yang, The recent development of vat photopolymerization: A review, Additive Manufacturing 48 (2021) 102423.
[52] E. Özkol, W. Zhang, J. Ebert, R. Telle, Potentials of the "Direct inkjet printing" method for manufacturing 3Y-TZP based dental restorations, Journal of the European Ceramic Society 32(10) (2012) 2193-2201.
[53] K. Shahzad, J. Deckers, Z. Zhang, J.-P. Kruth, J. Vleugels, Additive manufacturing of zirconia parts by indirect selective laser sintering, Journal of the European Ceramic Society 34(1) (2014) 81-89.
[54] S.L. Sing, W.Y. Yeong, Laser powder bed fusion for metal additive manufacturing: perspectives on recent developments, Virtual and Physical Prototyping 15(3) (2020) 359-370.
[55] D.-G. Ahn, Directed energy deposition (DED) process: State of the art, International Journal of Precision Engineering and Manufacturing-Green Technology 8 (2021) 703-742.
[56] J. Schweiger, D. Bomze, M. Schwentenwein, 3D printing of zirconia–what is the future?, Current Oral Health Reports 6 (2019) 339-343.
[57] R. Barros, F.J. Silva, R.M. Gouveia, A. Saboori, G. Marchese, S. Biamino, A. Salmi, E. Atzeni, Laser powder bed fusion of Inconel 718: residual stress analysis before and after heat treatment, Metals 9(12) (2019) 1290.
[58] J.P. Kruth, P. Mercelis, J. Van Vaerenbergh, L. Froyen, M. Rombouts, Binding mechanisms in selective laser sintering and selective laser melting, Rapid prototyping journal 11(1) (2005) 26-36.
[59] J.-P. Kruth, X. Wang, T. Laoui, L. Froyen, Lasers and materials in selective laser sintering, Assembly Automation 23(4) (2003) 357-371.
[60] E. Yasa, J.-P. Kruth, Application of laser re-melting on selective laser melting parts, Advances in Production engineering and Management 6(4) (2011) 259-270.
[61] I. Shishkovsky, I. Yadroitsev, P. Bertrand, I. Smurov, Alumina–zirconium ceramics synthesis by selective laser sintering/melting, Applied Surface Science 254(4) (2007) 966-970.
[62] P. Mercelis, J.P. Kruth, Residual stresses in selective laser sintering and selective laser melting, Rapid prototyping journal 12(5) (2006) 254-265.
[63] M.X. Gan, C.H. Wong, Properties of selective laser melted spodumene glass-ceramic, Journal of the European Ceramic Society 37(13) (2017) 4147-4154.
[64] A. Standard, F2792-12a: standard terminology for additive manufacturing technologies (ASTM International, West Conshohocken, PA, 2012), Procedia Eng 63 (2013) 4-11.
[65] W. Du, X. Ren, Z. Pei, C. Ma, Ceramic binder jetting additive manufacturing: a literature review on density, Journal of Manufacturing Science and Engineering 142(4) (2020) 040801.
[66] W. Du, M. Singh, D. Singh, Binder jetting additive manufacturing of silicon carbide ceramics: Development of bimodal powder feedstocks by modeling and experimental methods, Ceramics International 46(12) (2020) 19701-19707.
[67] E. Sachs, M. Cima, J. Cornie, Three-dimensional printing: rapid tooling and prototypes directly from a CAD model, CIRP annals 39(1) (1990) 201-204.
[68] S. Manotham, S. Channasanon, P. Nanthananon, S. Tanodekaew, P. Tesavibul, Photosensitive binder jetting technique for the fabrication of alumina ceramic, Journal of Manufacturing Processes 62 (2021) 313-322.
[69] S. Gaytan, M. Cadena, H. Karim, D. Delfin, Y. Lin, D. Espalin, E. MacDonald, R. Wicker, Fabrication of barium titanate by binder jetting additive manufacturing technology, Ceramics International 41(5) (2015) 6610-6619.
[70] A. Aversa, A. Saboori, E. Librera, M. de Chirico, S. Biamino, M. Lombardi, P. Fino, The role of Directed Energy Deposition atmosphere mode on the microstructure and mechanical properties of 316L samples, Additive Manufacturing 34 (2020) 101274.
[71] P. Colombo, J. Schmidt, G. Franchin, A. Zocca, J. Günster, Additive manufacturing techniques for fabricating complex ceramic components from preceramic polymers, Am. Ceram. Soc. Bull 96(3) (2017) 16-23.
[72] C. Suwanpreecha, A. Manonukul, A review on material extrusion additive manufacturing of metal and how it compares with metal injection moulding, Metals 12(3) (2022) 429.
[73] S.S. Crump, Apparatus and method for creating three-dimensional objects, Google Patents, 1992.
[74] A. Standard, Standard terminology for additive manufacturing technologies, ASTM International

F2792-12a (2012) 1-9.
[75] D. Ibrahim, T.L. Broilo, C. Heitz, M.G. de Oliveira, H.W. de Oliveira, S.M.W. Nobre, J.H.G. dos Santos Filho, D.N. Silva, Dimensional error of selective laser sintering, three-dimensional printing and PolyJet™ models in the reproduction of mandibular anatomy, Journal of Cranio-Maxillofacial Surgery 37(3) (2009) 167-173.
[76] G. Kim, Y. Oh, A benchmark study on rapid prototyping processes and machines: quantitative comparisons of mechanical properties, accuracy, roughness, speed, and material cost, Proceedings of the Institution of Mechanical Engineers, Part B: Journal of Engineering Manufacture 222(2) (2008) 201-215.
[77] T. Hafkamp, G. van Baars, B. de Jager, P. Etman, A feasibility study on process monitoring and control in vat photopolymerization of ceramics, Mechatronics 56 (2018) 220-241.
[78] J. Huang, Q. Qin, J. Wang, A review of stereolithography: Processes and systems, Processes 8(9) (2020) 1138.
[79] T.A. Otitoju, P.U. Okoye, G. Chen, Y. Li, M.O. Okoye, S. Li, Advanced ceramic components: Materials, fabrication, and applications, Journal of industrial and engineering chemistry 85 (2020) 34-65.
[80] R. Raj, Fundamental research in structural ceramics for service near 2000 C, Journal of the American Ceramic Society 76(9) (1993) 2147-2174.
[81] R. Riedel, G. Passing, H. Schönfelder, R. Brook, Synthesis of dense silicon-based ceramics at low temperatures, Nature 355(6362) (1992) 714-717.
[82] U. Chowdhry, A. Sleight, Ceramic substrates for microelectronic packaging, Annual review of materials science 17(1) (1987) 323-340.
[83] J.G. Drobny, Polymers for electricity and electronics: materials, properties, and applications, John Wiley & Sons2012.
[84] S. Ray, R.P. Cooney, Thermal degradation of polymer and polymer composites, Handbook of environmental degradation of materials, Elsevier2018, pp. 185-206.
[85] M. Nicholas, D. Mortimer, Ceramic/metal joining for structural applications, Materials Science and Technology 1(9) (1985) 657-665.
[86] M. Naser, Extraterrestrial construction materials, Progress in materials science 105 (2019) 100577.
[87] J.-W. Park, P. Mendez, T. Eagar, Strain energy distribution in ceramic-to-metal joints, Acta Materialia 50(5) (2002) 883-899.
[88] Y. Imanaka, Multilayered low temperature cofired ceramics (LTCC) technology, Springer Science & Business Media2005.
[89] M. Hołyńska, A. Tighe, C. Semprimoschnig, Coatings and thin films for spacecraft thermo-optical and related functional applications, Advanced Materials Interfaces 5(11) (2018) 1701644.
[90] H. Pattee, R.M. Evans, R.E. Monroe, Joining ceramics and graphite to other materials, Technology Utilization Division, Office of Technology Utilization, National …1968.
[91] C. Walker, J. Romero, R. Stokes, Active-brazed ceramic-tungsten carbide assemblies for seal applications, Microscopy and Microanalysis 17(S2) (2011) 1844-1845.
[92] K.H. Sandhage, H.J. Schmutzler, R. Wheeler, H.L. Fraser, Mullite Joining by the Oxidation of Malleable, Alkaline-Earth-Metal-Bearing Bonding Agents, Journal of the American Ceramic Society 79(7) (1996) 1839-1850.
[93] R. Do Nascimento, A. Martinelli, A. Buschinelli, Recent advances in metal-ceramic brazing, Cerâmica 49 (2003) 178-198.
[94] M. Yoshimura, W. Suchanek, In situ fabrication of morphology-controlled advanced ceramic materials by Soft Solution Processing, Solid State Ionics 98(3-4) (1997) 197-208.
[95] M. Haselman, S. Hauck, The future of integrated circuits: A survey of nanoelectronics, Proceedings of the IEEE 98(1) (2009) 11-38.
[96] L.-F. Wang, Z. Li, B.-A. Zhou, Y.-S. Duan, N. Liu, J.-X. Zhang, Study on Tungsten Metallization and Interfacial Bonding of Silicon Nitride High-Temperature Co-Fired Ceramic Substrates, Materials 16(7) (2023) 2937.
[97] J. Zhou, Towards rational design of low-temperature co-fired ceramic (LTCC) materials, Journal of Advanced Ceramics 1 (2012) 89-99.
[98] K.H. Cheah, K.-S. Low, Fabrication and performance evaluation of a high temperature co-fired ceramic vaporizing liquid microthruster, Journal of Micromechanics and Microengineering 25(1)

(2014) 015013.
[99] J. Raynaud, V. Pateloup, M. Bernard, D. Gourdonnaud, D. Passerieux, D. Cros, V. Madrangeas, T. Chartier, Hybridization of additive manufacturing processes to build ceramic/metal parts: Example of LTCC, Journal of the European Ceramic Society 40(3) (2020) 759-767.
[100] K.H. Rida, Packaging of microwave integrated circuits in LTCC technology, Télécom Bretagne, Université de Bretagne Occidentale, 2013.
[101] J. Raynaud, V. Pateloup, M. Bernard, D. Gourdonnaud, D. Passerieux, D. Cros, V. Madrangeas, P. Michaud, T. Chartier, Hybridization of additive manufacturing processes to build ceramic/metal parts: Example of HTCC, Journal of the European Ceramic Society 41(3) (2021) 2023-2033.
[102] M. Sebastian, H. Jantunen, High temperature cofired ceramic (HTCC), low temperature cofired ceramic (LTCC), and ultralow temperature cofired ceramic (ULTCC) materials, Microwave Materials and Applications 2V Set (2017) 355-425.
[103] R.B. Heimann, Classic and advanced ceramics: from fundamentals to applications, John Wiley & Sons2010.
[104] M.N. Rahaman, Ceramic processing and sintering, CRC press2017.
[105] K.V. Wong, A. Hernandez, A review of additive manufacturing, International scholarly research notices 2012 (2012).
[106] O. Abdulhameed, A. Al-Ahmari, W. Ameen, S.H. Mian, Additive manufacturing: Challenges, trends, and applications, Advances in Mechanical Engineering 11(2) (2019) 1687814018822880.
[107] J.A. Fernie, R. Drew, K. Knowles, Joining of engineering ceramics, International Materials Reviews 54(5) (2009) 283-331.
[108] C. Cui, Q. Ding, S. Yu, C. Yu, D. Jiang, C. Hu, Z. Gu, J. Zhu, Strategies to break the trade-off between infrared transparency and conductivity, Progress in Materials Science (2023) 101112.
[109] P. Sturesson, Z. Khaji, L. Klintberg, G.J.I.S.J. Thornell, Ceramic pressure sensor for high temperatures–investigation of the effect of metallization on read range, 17(8) (2017) 2411-2421.
[110] F. Suarez, A. Nozariasbmarz, D. Vashaee, M.C.J.E. Öztürk, E. Science, Designing thermoelectric generators for self-powered wearable electronics, 9(6) (2016) 2099-2113.
[111] W.D. Callister Jr, Materials science and engineering an introduction, 2007.
[112] M.D. Bartlett, S.W. Case, A.J. Kinloch, D.A. Dillard, Peel tests for quantifying adhesion and toughness: A review, Progress in Materials Science 137 (2023) 101086.
[113] D. Yu, R. Hensel, D. Beckelmann, M. Opsölder, B. Schäfer, K. Moh, P.W. de Oliveira, E. Arzt, Tailored polyurethane acrylate blend for large-scale and high-performance micropatterned dry adhesives, Journal of materials science 54 (2019) 12925-12937.
[114] D. Seo, S. Park, J. Lee, Sinterability and conductivity of silver paste with Pb-free frit, Current Applied Physics 9(1) (2009) S72-S74.
[115] S. Yao, J. Xing, J. Zhang, S. Xiong, Y. Yang, X. Yuan, H. Li, H. Tong, Microscopic investigation on sintering mechanism of electronic silver paste and its effect on electrical conductivity of sintered electrodes, Journal of Materials Science: Materials in Electronics 29 (2018) 18540-18546.
[116] X.-L. Liu, Y. Zhao, W.-J. Wang, S.-X. Ma, X.-J. Ning, L. Zhao, J.J.I.S.J. Zhuang, Photovoltaic self-powered gas sensing: A review, 21(5) (2020) 5628-5644.
[117] T.F. Chen, K.S.J.J.o.a. Siow, Compounds, Comparing the mechanical and thermal-electrical properties of sintered copper (Cu) and sintered silver (Ag) joints, 866 (2021) 158783.
[118] M. Alhendi, F. Alshatnawi, E.M. Abbara, R. Sivasubramony, G. Khinda, A.I. Umar, P. Borgesen, M.D. Poliks, D. Shaddock, C.J.A.M. Hoel, Printed electronics for extreme high temperature environments, 54 (2022) 102709.